International Journal for Multidisciplinary Research (IJFMR)
E-ISSN: 2582-2160 ● Website: www.ijfmr.com ● Email: editor@ijfmr.com

Ferrites for Permanent Magnet and Microwave Devices Applications: A Review

Yaseen Mohd[1], Deepika Sharma[2], Sonia Khan[4], Indu Sharma[2,3*]

[1]Center for Green Energy Research, Department of Physics, CPU, Hamirpur, Himachal Pradesh 176041, India
[2]Department of Physics, Himachal Pradesh University, Shimla, 171005, India
[3]Centre for Green Energy and Nanotechnology,Himachal Pradesh University, Shimla, 171005, India
[4]Institute of Vocational (Tourism) Studies, Himachal Pradesh University, Shimla, 171005, India
*Corresponding Author Details: induphyhmr@gmail.com

Abstract
Hard ferrite, especially hexaferrite, has the advantages of low cost, high chemical stability, excellent corrosion resistance, and desirable magnetic properties, and is widely used. This review paper gives an overview of the structural and magnetic properties, synthesis processes, and applications of hard ferrites. The crystal structure, coercivity, magnetocrystalline anisotropy, and permanent magnet performance of various hexaferrite families are discussed. The effects of chemical doping, hard-soft magnetic material exchange coupling, and nanostructuring on the magnetic properties are also highlighted. The role of various synthesis methods, such as sol-gel and citrate precursor methods, has been reviewed. The paper presents the application of hard ferrite in a variety of fields, such as permanent magnets for electrical vehicle, microwave devices, and electromagnetic interference shielding. Such development also contributes to smart and sustainable tourism by enhancing the transportation, communication, and technological aspects of the environment.

Keywords: M-type ferrite, magnetic properties, Synthesis method, Permanent magnets, Microwave absorption.

1. Introduction :

With its substantial impacts on the world's GDP, jobs, and international trade, the tourism industry is now recognized as the largest economic sector in the world. The large-scale expansion of tourism has led to serious issues related to resource depletion, sustainability, and climate change. Now, it has become essential to recognize the importance of knowing how tourism development can help achieve green growth goals [1–3]. One way to combine the idea of tourism with the use of green energy sources is to use cheap, easily available, non-hazardous, and eco-friendly magnetic materials. The purpose of this review paper is to deal with two important problems related to the environment: the use of costly and rare-earth permanent magnet (PM) in electrical vehicle (EVs) and electromagnetic interference (EMI) in telecommunications [4,5]. Batteries and motors are two essential components for the working of EVs. In recent years, scientists have been looking for an alternative to EV motors without the need for rare earth elements (REE) [6]. On the other hand, a large number of wireless devices and communications equipment operate on various frequencies, so it becomes essential to use some microwave (mW) absorbers to reduce EMI [5]. Ferrite nanoparticles (NPs) are pointed out as a probable material with an exceptional combination of magnetic

and dielectric properties to successfully address both challenges. Ferrites' exceptional magnetic behaviour has garnered a lot of interest [7]. These materials are valuable in magnetic energy conversion, information storage, spintronics, mW technology, PM for EVs, and EMI shielding, due to low cost, excellent stability, high electrical resistivity, and their magnetic properties, including high H_c and large crystalline anisotropy These materials are valuable in magnetic energy conversion, information storage, spintronics, mW technology, PM for EVs, and electromagnetic interference (EMI) shielding, due to low cost, excellent stability, high electrical resistivity, and their magnetic properties, including high coercivity and large crystalline anisotropy [8–11]. Ferrites are classifiable into various types, depending on the nature of their crystal structure and magnetic properties. Classification of ferrites is based on their crystal structure, such that there are spinel, garnet, ortho, or hexagonal ferrites. In addition, ferrites are categorized based on their magnetic properties into two groups, namely, hard ferrite (HF) and soft ferrite (SF) [11].

1.1. Ferrites

A consequence of their chemical composition and crystal structure, which will be discussed in more detail later, ferrites are a class of materials that indicate a unique combination of electrical and magnetic characteristics that make them extremely useful in a variety of applications. Unlike many other magnetic materials that are electrically conductive, ferrites are typically insulators or semiconductors, making them suitable for applications where minimizing eddy current losses is crucial. The versatility of ferrites stems from their ability to be tailored for specific functionalities in a variety of technological domains through controlled variations in their composition and processing methods. Ferrites have a basic quality in common with ferromagnetic materials, such as iron, cobalt, and nickel: they automatically become magnetic when the temperature drops below the Curie point. In the absence of a magnetic field from the outside, this spontaneous magnetization occurs due to the alignment of atomic magnetic moments beneath the material. Ferrites exhibit ferrimagnetism, a more complex magnetic arrangement than ferromagnets, where all magnetic moments align uniformly. Because the magnetic moments of different sublattices in the crystal structure of ferrimagnetic materials point in opposite directions, the net magnetic moment of these materials is often lower than that of a ferromagnet of the same composition. A major determinant of ferrites' magnetic characteristics, including their saturation magnetization (M_s), coercivity (H_c), and permeability (μ_r), is their ferrimagnetic behavior. One important factor influencing the magnetic properties of ferrites, such as saturation magnetization, coercivity, and permeability, is their ferrimagnetic behaviour. Although the ferrite family is mostly classified as spinel, garnet, and hexagonal ferrites (HgF), it contains a wide variety of structural shapes. Each of these types has unique magnetic characteristics and crystal structures [12]. Possibly the most common variety of ferrite, spinel ferrites have a cubic crystal structure and are utilized in magnetic recording media, transformers, and inductors. Having a cubic structure as well, garnet ferrites are especially well-suited for mW applications due to their exceptional resistance and low losses at high frequencies. Because of its layered hexagonal structure and significant magnetic anisotropy, HgF is ideal for PM applications and high-frequency devices. Many magnetic and electrical devices depend on these ferrite types due to their diverse properties.

1.2. Historical Context and Discovery

The discovery of hexagonal ferrites in the 1950s was a major turning point that sparked growing attention because of their significance in both commerce and technology [13] These materials created new opportunities for use in magnetic recording media, high-frequency devices, and PM due to their distinctive layered structure and strong magnetic anisotropy. The identification of hexaferrites not only increased the variety of magnetic materials that were accessible but it also prompted more investigation into the

fundamental properties of ferrites and their potential technological applications. The continued interest in and study of HFs underscore their significance in modern materials science and engineering.

Ideally suited engineering applications were highlighted in the description of manganese-zinc ferrite's mechanical and magnetic properties [14]. This preliminary study provided valuable insights into the possible use of ferrites in various devices and systems. High permeability, low losses, and exceptional mechanical strength are some of their attributes that are explained. Ferrites have become widely used in the electronics industry as a result of the discovery of appropriate engineering uses, such as filter coils and high-frequency transformers.

Ferrites have been used in filter coils and high-frequency transformers [14]. These applications take advantage of ferrites' unique combination of high permeability and low electrical conductivity. Ferrites are used in filter coils to increase inductance and improve circuit selectivity. Ferrite is utilized as the core material in high-frequency transformers to reduce eddy current losses and increase transformer efficiency. The use of ferrites in various applications has enabled the development of more compact, effective, and high-performance electrical devices. The basic chemical makeup of ferrites and the thermal treatments they undergo during manufacturing are intricately linked to their properties. The kind and concentration of magnetic ions present in the material, which is defined by its chemical composition, have a direct impact on the strength of magnetic interactions and, as a result, magnetic characteristics [15]. Heat treatments such as sintering and annealing control the microstructure of the ferrite, including grain size, density, and phase purity, all of which have a significant impact on its electrical and magnetic behaviour. Customizing ferrites' properties to meet the specific needs of different applications necessitates precise control over both the chemical composition and the thermal treatment.

In the PM industry, hard ferrites, particularly M-type hexagonal ferrites like strontium ferrite (SrF) and barium ferrite (BaF), occupy a major position due to their low cost and strong magnetic properties [16]. These materials provide unique electrical and magnetic properties that are useful in a variety of technical fields, making them essential in memory and mWshielding devices as well [17,18]. The properties, processing, uses, and developments of hard ferrites will be covered in this introduction, with an emphasis on their use in memory devices and PMs.

Hard ferrites, also known as ceramic magnets, are a type of PM made from iron oxide combined with barium, strontium, or cobalt. These magnets are not only inexpensive and robust, but they also possess unusual magnetic characteristics that make them suitable for memory devices. Hard ferrites can dependably retain magnetic information because of their high coercivity, which means they resist losing magnetism even under adverse situations such as heat or external magnetic fields. This stability is critical for memory devices, such as magnetic recording media used in old-school hard drives or magnetic tapes, where data must be safely preserved for extended periods of time. Furthermore, hard ferrites are resistant. It is anti-corrosion and can be molded into ultrafine particles, making it excellent for high-density storage solutions. Their ability to magnetize in certain patterns assists in the accurate writing and understanding of information. Hard ferrites, which are made from common and low-cost materials, provide a cost-effective solution for modern motor technology, combining performance and practicality in functions that need long-term data retention.

Both PMs and memory devices rely heavily on hard ferrites, a type of magnetic material. These materials have a unique mix of qualities that make them appropriate for a wide range of technological applications, including high coercivity and remanence (M_r) (a material's capacity to sustain magnetization) [17]. Hard ferrites, also known as hexaferrites, are ferrimagnetic oxides that are widely used in PMs in EVs and

memory devices because of their high coercivity, stability, and low cost. This in-depth examination delves into its basic qualities, recent advances, and prospects of hard ferrites, with a specific focus on their importance in the evolution of magnetic technology.

Ferrites, also known as magnetic oxide, have been utilized for hundreds of years, originating with loadstones (magnetite) for navigation in ancient Greece around 800 B.C. Early navigators used loadstones to determine magnetic north, demonstrating their original technical importance. William Gilbert conducted the first magnetism-related scientific investigation in 1600, while Hans Christian Oersted identified the link between electric current and magnetic field in 1819. There are two types of ferrites: soft and hard.

2. Classification of ferrites

Ferrites may be divided into two groups: those based on magnetic fields and those based on crystalline structure. Under the category of crystalline structure, there are four subtypes: garnet ferrite, ortho ferrite, spinal ferrites, and hexagonal ferrites. However, there are only two subtypes of ferrite, namely soft and hard, which are dependent on the characteristics of the magnetic field. Compared to soft ferrites, hard ferrites have greater magnetic properties.

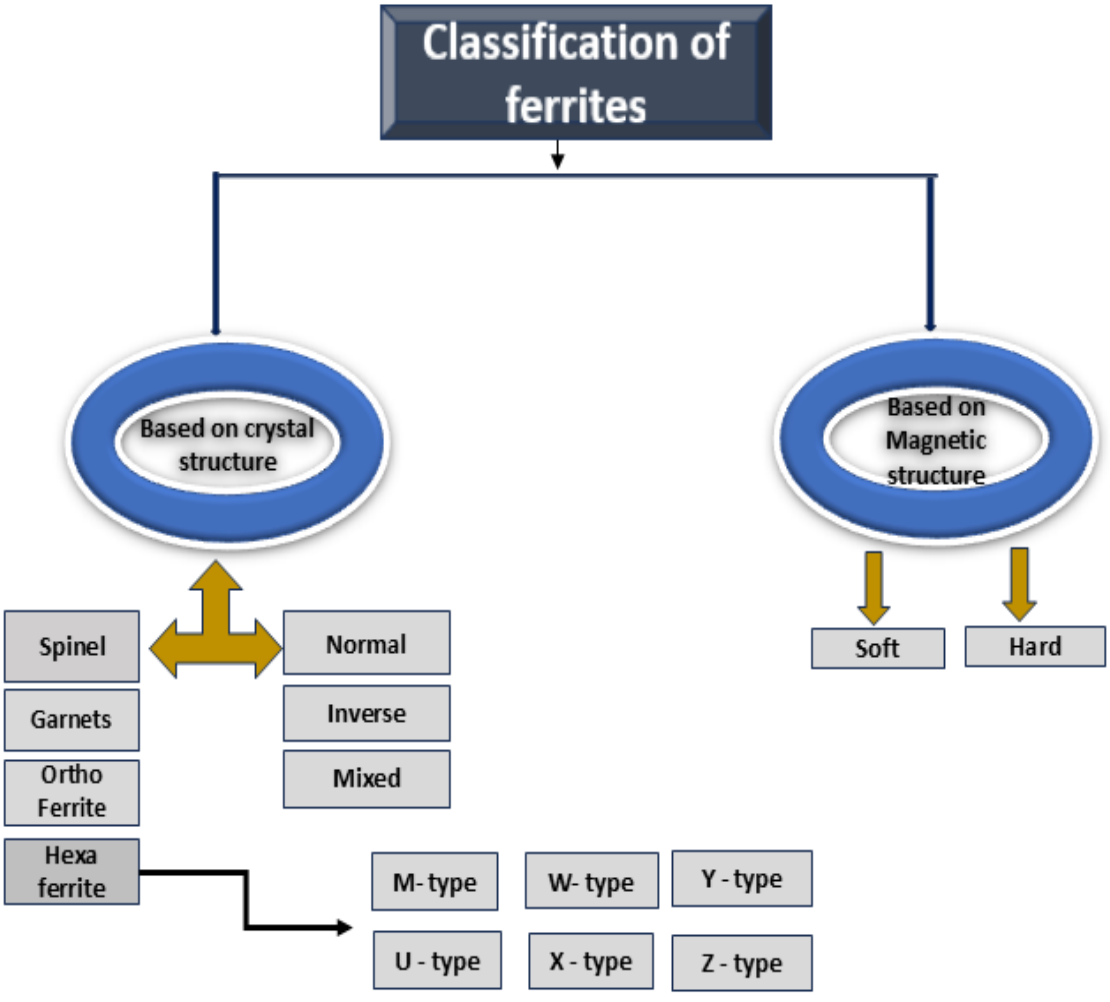


Fig.1: Classification of ferrites.

2.1 Soft Ferrites:

Soft ferrites, typically man-made, vary in size and shape and exhibit low coercivity, as shown in Fig. 1, making them easily magnetizable and ideal for use as conductors in magnetic fields. High-frequency applications require them, which are mostly made of garnets and spinels. Soft ferrites, especially spinel ferrites, were discovered in 1946 by J. L. Snoek at Philips Research in the Netherlands. They have low coercivity, a high squareness ratio, an important magneto-crystalline anisotropy, and strong Ms[19]. Soft ferrites have a small value of coercivity; therefore, they can be easily demagnetized.

2.1.1 Spinel Ferrites (SFs)

Spinel ferrites, along with hexagonal ferrites (HFs), are experiencing rapid growth in usage across various applications [20]. This surge in popularity is attributed to their flexible magnetic properties, ease of synthesis, and affordability. Their applications span a wide range of fields, such as transformers, pollution control, catalysis, pigments, electronic devices, gyromagnetic devices, medical devices, information storage, mobile communication, magnetic shielding, magnetic biosensors, and magnetic recording devices. The ability to tailor the properties of spinel ferrites through compositional modifications and controlled processing makes them attractive materials for both traditional and emerging technologies.

Spinel ferrites, represented by the general formula MFe_2O_4 (where M can be Co, Ni, Cu, Mg, or Zn), can be synthesized using sucrose auto-combustion [21]. This technology provides a straightforward and effective way to create nanocrystalline ferrite powders with precise particle size and excellent purity. Sucrose serves as both a fuel and a complexing agent, allowing for more homogenous mixing of metal ions and promoting the spinel structure to form when burned. The resultant powders can be further treated, such as sintering, to produce dense ceramic materials with the necessary magnetic characteristics.

Identification techniques such as X-ray diffraction are critical for determining the formation purity and crystallite size of synthetic ferrites. The diffraction patterns acquired from XRD measurements may be compared to standard reference patterns to determine the presence of the spinel phase and its lattice characteristics. The size of a crystallite can be determined by applying the Scherrer equation to the broadening of diffraction peaks. XRD is an important tool for quality control and understanding the relationship between synthesis conditions and spinel ferrites' structural properties.

Classification of Spinel Ferrite Spinel ferrites may be classified into two types depending on the arrangement of their two cationic regions: trivalent ferric ions and divalent metal ions which is shown in Fig.2 below..

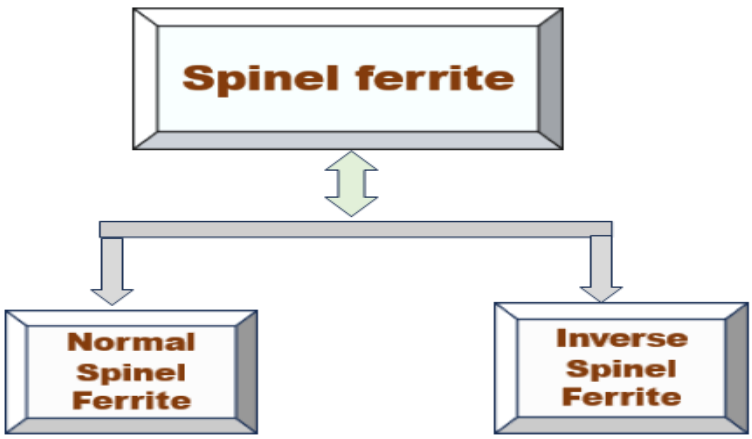


Fig.2: Spinel Ferrite Classification

2.1.2 Spinel-ferrite structure :

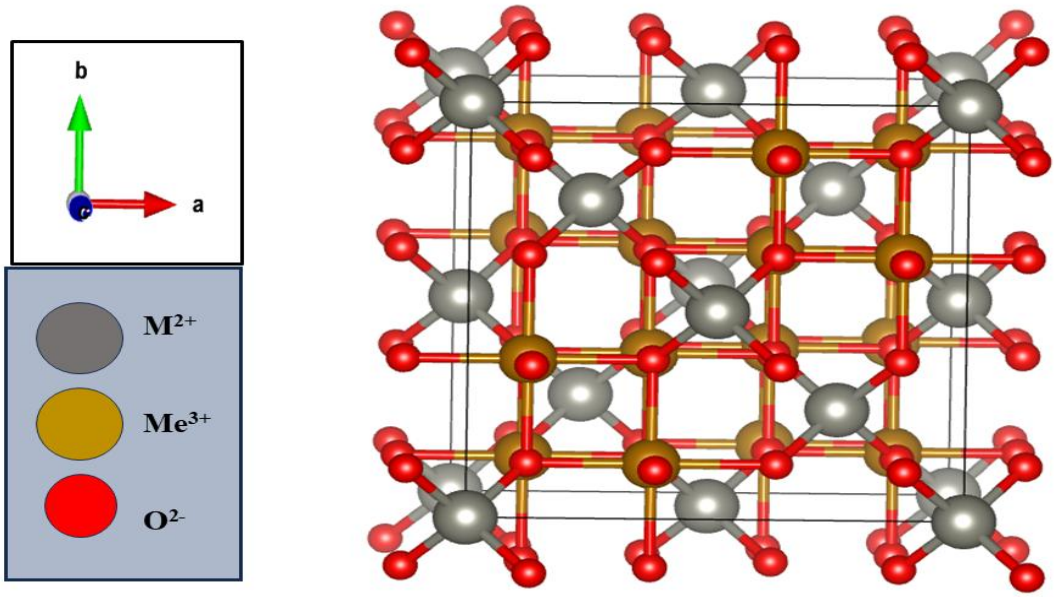


Fig. 3: Spinel-ferrite crystal structure [22]

Spinel ferrite has a cubic close-packed structure and a unit cell of 8 formula units ($M_8Fe_{16}O_{32}$) with metal ions occupying 1/8 of the tetrahedral and 1/2 of the octahedral sites. In normal spinal ferrites, the structure of AB_2O_4, where the trivalent Fe^{3+} ion occupies octahedral sites, and the divalent A^{2+} ion occupies tetrahedral sites. In the case of inverse spinel ferrite, the divalent ions occupy the iron-vacant octahedral places, but the Fe^{3+} ions are evenly distributed in octahedral and tetrahedral sites (like $NiFe_2O_4$) [23], as shown in the Fig. 3.

2.2 Hard Ferrites:

Hexaferrites, another name for hard ferrites, are ferrimagnetic oxides possessing a hexagonal magneto-plumbite-type crystal structure. They are useful due to their high electrical resistivity, high magnetic permeability, and tenable permittivity. Additionally, HFs have minimal eddy current loss at high frequencies, good mechanical hardness, and outstanding chemical stability [17]. These materials gained prominence in the 1950s and have since been extensively utilized in PMs, recording media, storage devices, rod antennas, and high-frequency mW devices, among other applications [13].

2.2.1 Classification of hard ferrites :-

(a) Garnet Ferrites

Garnet ferrites are another significant class of ferrite materials [12]. These ferrites, which have a cubic crystal structure similar to the mineral garnet, are suitable for a wide range of specialized applications due to their particular magnetic and optical properties. In contrast to spinel and hexagonal ferrites, garnet ferrites generally include rare earth ions in their crystal structure, which contributes to their peculiar magnetic behavior. They are highly resistive and have minimal dielectric losses at mW frequencies, making them ideal for use in optical isolators and mW devices.

Eddy current effects provide size-dependent contributions in polycrystalline ferrites and garnets. Circulating currents, known as eddy currents, are created in materials by a fluctuating magnetic field and can cause significant energy losses at high frequencies. The extent of these losses is determined by the electrical conductivity of the material, as well as the diameters and shape of its crystallites. It is possible

to minimize eddy current losses and improve high-frequency performance by modifying the ferrite microstructure, such as lowering grain size or increasing resistivity.

Anisotropy and porosity have been associated with size-independent contributions [12]. Magnetic anisotropy refers to the tendency of magnetization to align along certain crystallographic orientations, as well as the material's coercivity and the shape of the hysteresis loop. Porosity, or the presence of voids or pores inside a material, may also affect magnetic characteristics by lowering the effective volume of magnetic material and producing demagnetizing fields. Controlling and optimising ferrites' magnetic properties for specific applications necessitates consideration of these issues.

(b) Hexagonal Ferrites (HFs)

HFs are becoming more popular in applications such as PMs, recording media, storage devices, rod antennas, and high-frequency mW devices. This is owing to their strong magnetic anisotropy, high Curie temperatures, and chemical stability. Their use in high-frequency devices is particularly remarkable since they can function at frequencies that regular spinel ferrites cannot. Because of their versatility, HFs are essential components in many modern technologies.

Hexaferrites are classified into six types: M, Z, Y, X, U, and W. Because of their different magnetic properties and crystal structures, each kind is suitable for a wide range of applications. M-type HFs, such as SrF ($SrFe_{12}O_{19}$) and BaF ($BaFe_{12}O_{19}$), are commonly employed as PMs due to their strong H_c and M_r. The additional forms of HF provide a spectrum of magnetic and dielectric properties that may be adjusted for specific applications in mW devices and magnetic recording media. The most commonly produced HFis Barium M-type ferrite (BaF) [13]. Its abundance, low cost, and excellent magnetic characteristics make it a preferred choice for PM applications in automotive, consumer electronics, and industrial equipment. BaF is also used in mW devices such as circulators and isolators because of its high magnetic anisotropy and minimal loss at high frequencies. The broad usage of BaM demonstrates its relevance as a crucial material in current magnetic technology.

Types and Structures of HFs:

Hexaferrites are classified into six types: M, Z, Y, X, U, and W. The barium M-type ferrite is the most extensively produced worldwide. Each category demonstrates ferrimagnetic behavior that is intimately connected to its crystal structure [13].

Sr no.	Types	Chemical Formula	Stacking	Key Properties	Main Applications
1.	Spinel ferrites	2 $MeO{\cdot}2Fe_2O_3$	-	Good catalytic activity, large surface area	Motors, loudspeakers Magnetic stripes
2.	z-type ferrites	$3BaO{\cdot}2MeO{\cdot}12Fe_2O_3$	RSTSR*S*T*S*	Soft magnetic character, acceptable high frequency	Automotive motors, sensors, Magnetic separators
3.	W – Type Ferrites	$2BaO{\cdot}2MeO{\cdot}6Fe_2O_3$	RSSR*S*S*	Large crystalline anisotropy	MWdevices, advanced magnetic components

4.	M-Type Ferrites	$BaO{\cdot}6Fe_2O_3$	RSR*S*	High curie temperature, High chemical stability, low cost	Wide range of PMs
5.	Y-Type Ferrites	$2BaO{\cdot}2MeO{\cdot}6Fe_2O_3$	TSTSTS	Lower H_c, suitable for high -frequency use, planar anisotropy	mW device, high-frequency applications
6.	U-type ferrites	$Ba_4Me_2Fe_{36}O_{60}$	SRS*R*S*T	High electric resistivity, low cost and chemical stability.	PMs and switching devices.
7.	x-type ferrites	$2BaO{\cdot}2MeO{\cdot}14\ Fe_2O_3$	RSR*S*S*	High curie temperature, high chemical stability	PMs, mW devices

Table 1: Types of hexaferrites [24]

3. Stacking Sequence (S, R, and T)

S-block: with the chemical formula $Me_2Fe_4O_8$, consists of two hexagonal, closely spaced oxygen layers.

R-block: This block is a three-layer oxygen structure composed of $BaFe_6O_{11}$ or $SrFe_6O_{11}$, with a Ba^{2+} or Sr^{2+} ion substituted for one of the intermediate layer's oxygen ions.

T- block: The oxygen ion is replaced by one Ba^{2+} or Sr^{2+} ion. In each of the two intermediate layers of this block's four oxygen layers. Either $Ba_2Fe_8O_{14}$ or $Sr_2Fe_8O_{14}$ is the chemical formula.

3.1 Crystal Structure of Hard Ferrites

Hard ferrites typically adopt a hexagonal crystal structure, which is key to their magnetic properties. The main structural types are:

Magnetoplumbite Structure (M-type)

The most prevalent structure for $BaFe_{12}O_{19}$, $SrFe_{12}O_{19}$, and $PbFe_{12}O_{19}$ is M-type hexaferrite, as shown in Fig. 4. It is composed of a close-packed hexagonal lattice of hexagonal (R) and spinel-like (S) pieces that alternate. The five crystallographic positions that Fe^{3+} ions inhabit are tetrahedral, octahedral, and trigonal bipyramidal. In its unit cell, which has two formula units (36 atoms). Anti-parallel spin alignments of A net magnetic moment has been generated along the c-axis by Fe^{3+} ions, which makes M-type HFs ferrimagnetic. Strong H_c is a result of significant magneto crystalline anisotropy, making it perfect for PMs [25].

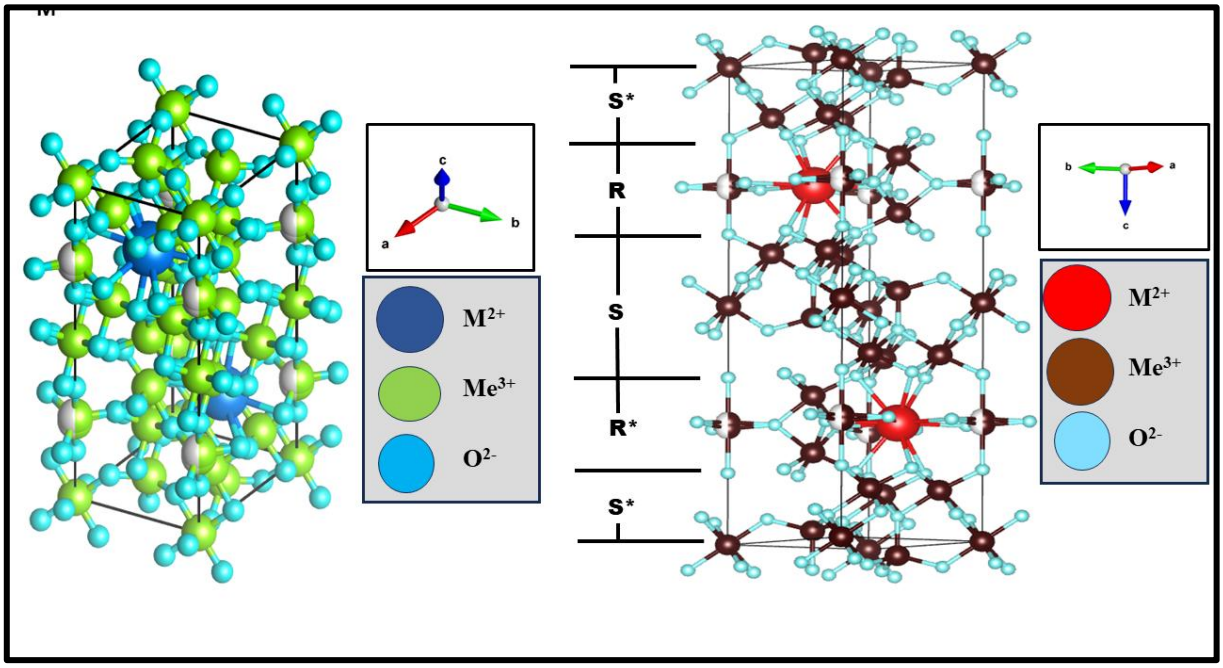
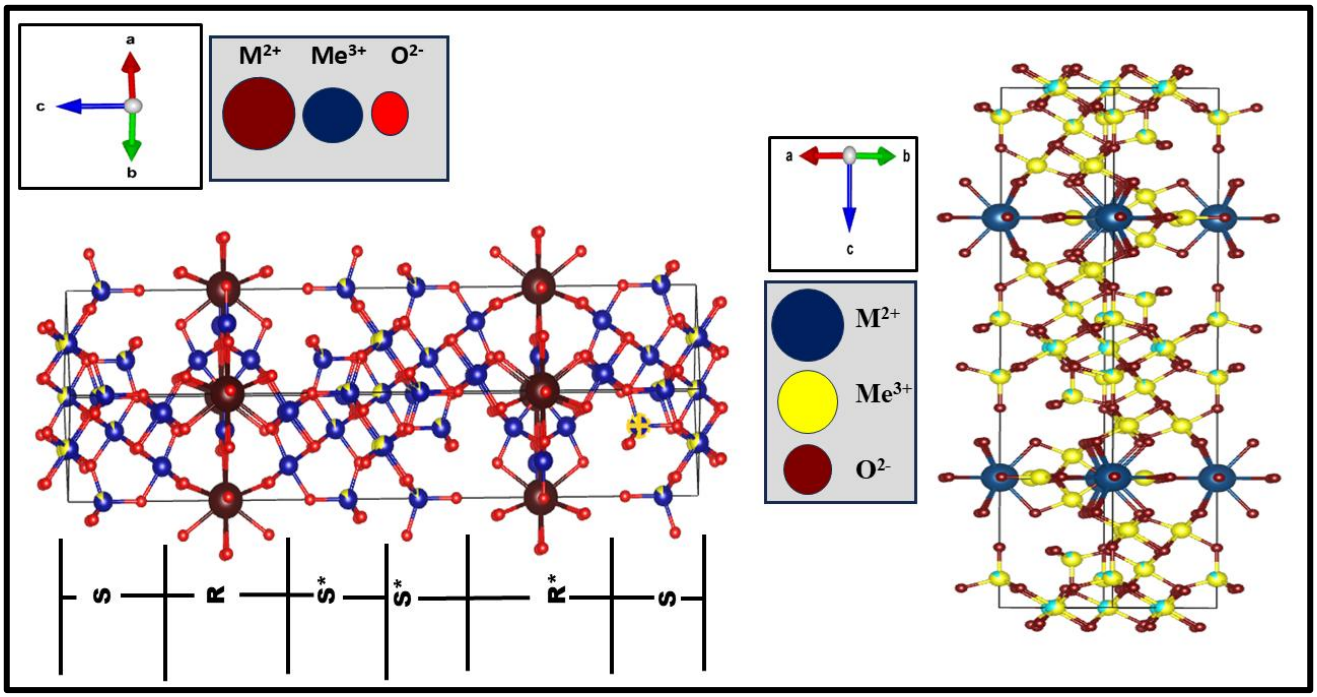


Fig.4. Crystal structure of M-type HF [13]

W-type Structure

Me is usually a first row transition metal or another divalent cation, and the formula for w ferrites is $BaMe_2Fe_{16}O_{27}$. It is possible to substitute another group two metal for the barium.

Fig 5 : W-type HF crystal structure [13]



Though first only created as a mixed phase with Mand X ferrites, Fe2W ($BaFe_2Fe_{16}O_{27}$) was the first W ferrite to be reported. Even though the c-axis of the hexagonal crystal structure had an easy axis of magnetization, single-phase Fe2W had a much higher electrical conductivity than BaM because of the Fe^{2+} ion *[26]*.

The W-type Ferrite figure is shown in Fig. 5

Y-type Structure

Hexagonal M-type and cubic spinel ferrites make up Y-type ferrites as shown in Fig. 6 below. It was discovered that the simplest plane of spontaneous magnetism at room temperature in Y-type hexaferrites is the basal c-plane, which is perpendicular to the c-axis. Y-type are work well for use at ultra high frequencies in modern information and communication processing devices. To study magnetoelectric and mW device applications, the majority of Studies on Y-type HF have concentrated on its magnetic and structural properties *[27]*.

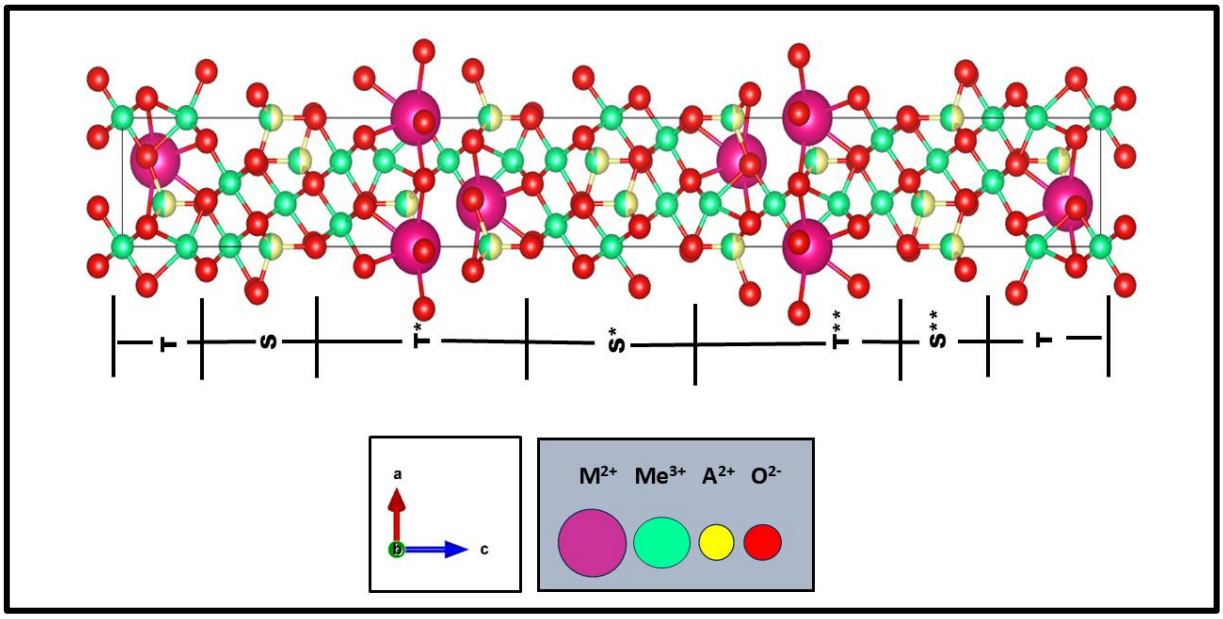


Fig. 6: Crystal structure of Y-type hexaferrite[13]

U-type structure:

Block stacking structure SRS*R*S*T is created when Z+M type HF and U type HF are combined. Undoubtedly, the most complicated magneto plumbite, U-type hexaferrites, have the longest unit cell. Because of their maximum inherent magnetocrystalline anisotropy (MCA) and maximal complexity, U-type hexaferrites have demonstrated greater mW absorption over a broad frequency range.

X-type Structure:

Me is an acronym for divalent metal ion, and its chemical formula is $Ba_2Me_2Fe_{28}O_{46}$ as shown in Fig. 7. In this structure, three oxygen layer blocks R ($BaFe_6O_{11}$) and S (Fe_6O_8) consist of $BaFe_6O_8$ and $BaFe_6O_{11}$. Six R and S blocks are arranged along the hexagonal c axis in the model SRS*S*S*R*. Four hexagonally stacked layers of M and W type structure make up the unit cell in R3m space symmetry.

Fig 7: X- type crystal structure of hexaferrite[13]

Z-Type Structure: Z hexaferrites can be obtained by combining M ($BaFe_{12}O_{19}$) and Y ($Ba_2Me_2Fe_{12}O_{22}$) hexaferrites, as shown in Fig 8. The crystal structure includes 33 layers located on a hexagonal c-axis and classified into S, R, and T blocks, which correspond to the S, R, and T Blocks models, according to the STSR block-based model.

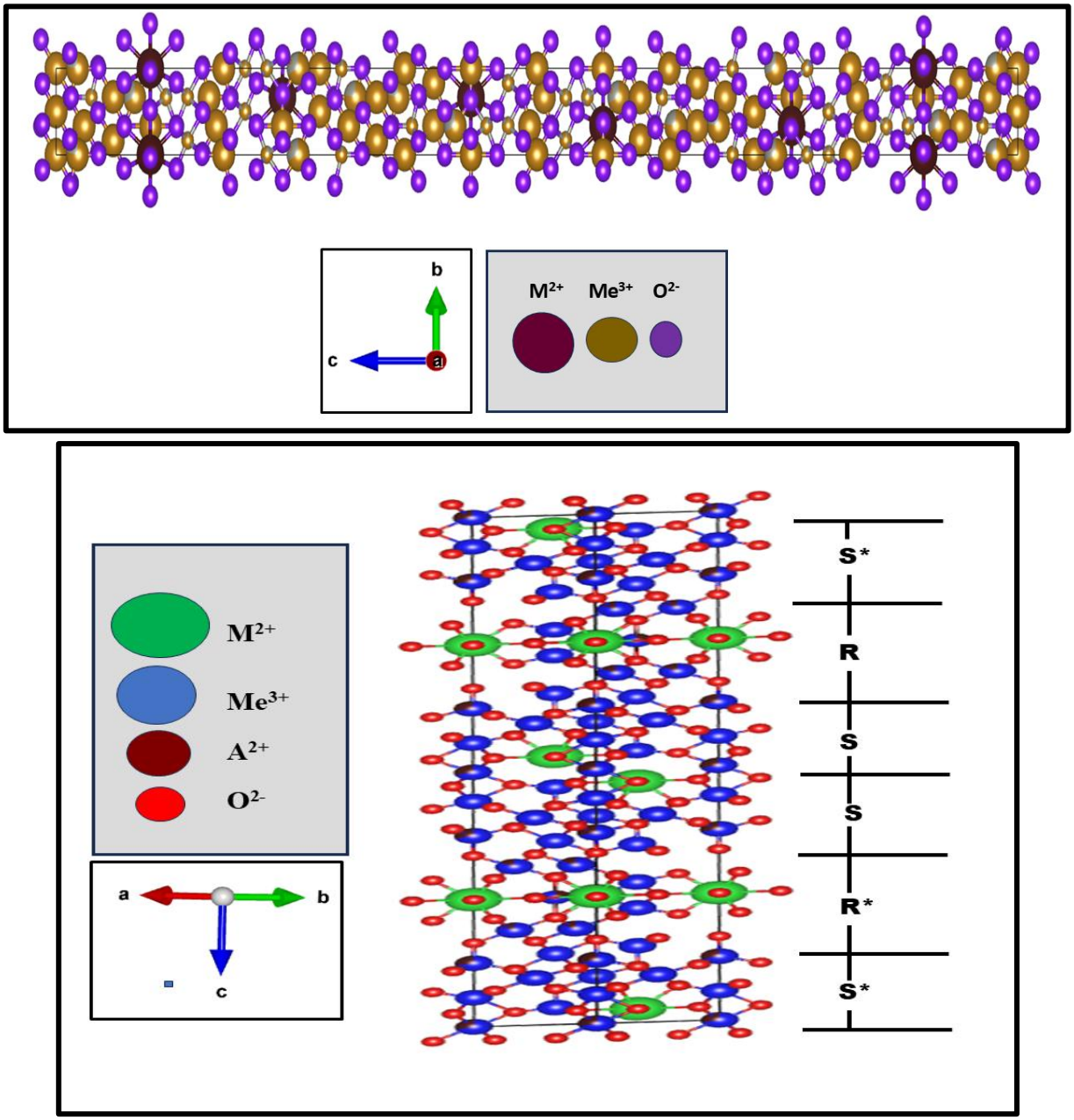


Fig.8: Crystal structure of Z type HF[13]

4. Fundamental Properties of Hard Ferrites

Hard ferrites, also known as hexaferrites, are ferrimagnetic oxides with a hexagonal magneto-plumbite-type crystal structure [17]. Their desirable characteristics make them suitable for many potential applications [24] . The general chemical formula for M-type hexaferrites is $BaFe_{12}O_{19}$ or $SrFe_{12}O_{19}$ [28], where barium or strontium can be substituted with other components to alter their magnetic properties [29]. Their substantial uniaxial magnetocrystalline anisotropy is the main cause of these materials' high H_c., i.e., resistance to demagnetization [30].

Intrinsic and Extrinsic Properties

Internal and external factors impact the magnetic properties of hard ferrites. The material's crystal structure and chemical composition provide intrinsic properties such as magnetocrystalline anisotropy, Curie temperature (T_c), and M_s[31]. Extrinsic characteristics, including density, orientation, shape, and grain

size, are related to the material's microstructure [32]. These two sets of features have a significant impact on the overall performance of hard ferrites in a range of applications.

4.1. Magnetic Properties

Hard ferrites have numerous essential magnetic properties that contribute to their popularity in PM applications. These are:

High Coercivity (H_c): The capacity to resist demagnetization is crucial for PMs, and hard ferrites have high H_c values that vary from 200 to 400 kA/m [33].

Moderate Remanence (M_r): M_r is the residual magnetization left behind when an external magnetic field is removed. Hard ferrites have modest M_r values, which contribute to their capacity to produce a magnetic field [34].

The Curie temperature (T_c) is the point at which a material loses its ferromagnetic properties. Hard ferrites have high Curie temperatures, which often surpass 700 K, assuring their stability at high temperatures [31].

Energy Product $(BH)_{max}$: is a measure of a PM's strength, indicating the maximum energy stored in the magnetic field. Although hard ferrites provide less energy than rare-earth magnets, their other benefits make them useful for a variety of applications [35].

Advantages of Hard Ferrites

Hard ferrites have various benefits over other PM materials.

Low Cost: Because hard ferrites are created from abundant and inexpensive raw materials, they provide an affordable alternative to rare-earth magnets [30].

High Availability: Hard ferrites' raw materials are readily available, reducing the possibility of supply chain disruption [30].

Excellent Chemical Stability: Hard ferrites are highly resistant to corrosion and oxidation, ensuring long-term performance in a variety of settings [13].

Low Eddy Current Losses: Due to their high electrical resistivity, hard ferrites offer small eddy current losses at high frequencies, making them appropriate for high frequency applications [13].

Chemical Doping

Foreign ions can be introduced into the crystal structure of hard ferrites, altering their magnetic properties. Doping can influence the material's magneto crystalline anisotropy, saturation magnetization, and Curie temperature [36]. Some popular dopants include:

Aluminium (Al) : doping reduces saturation magnetization but increases H_c in hexaferrites [36].

Cobalt (Co): By substituting cobalt ions for iron ions, hexaferrites' magneto-crystalline anisotropy and Hc can be increased [37].

Lanthanum (La) substitution improves the sintering behavior and grain alignment of hexaferrites, resulting in improved magnetic properties [38].

Gadolinium (Gd) can change the structural, thermodynamic, and magnetic properties of $SrFe_{12}O_{19}$ HF[39].

Hard-Soft Magnetic Composites

Combining hard ferrites and soft magnetic materials can result in exchange-spring magnets with higher energy output. The hard ferrite phase has significant Hc, whereas the soft magnetic phase leads to saturation magnetization [32]. The exchange coupling between the two phases leads to increased overall magnetic performance. Examples of hard-soft ferrite composites include.

$Zn_{0.2}Fe_{2.8}O_4/SrFe_{12}O_{19}$; which combines zinc and strontium ferrites to optimize energy output [32].
$SrFe_{12}O_{19}/NiFe_2O_4$: Strontium ferrite and nickel ferrite combine to improve magnetic characteristics [40].
$BaFe_{12}O_{19}/CoFe_2O_4$: BaFis mixed with cobalt ferrite to produce a high energy product [40].

5. Ferrite Synthesis Methods

Ferrite materials are well-known for their unique electrical and magnetic properties, which have made them widely used in a variety of technical applications. These materials are commonly used in mW devices because of their high magnetic permeability, and electrical resistivity is critical for performance [17]. Furthermore, ferrites serve as both PMs and high-density recording mediums, resulting in efficient data storage and steady magnetic fields for a wide range of applications. Ferrites' versatility extends to biomedical applications; spinel ferrites are used in electrical devices, medication delivery systems, and magnetic resonance imaging (MRI) [40]. Furthermore, certain ferrites, such as tin ferrite ($SnFe_2O_4$), have properties that make them suitable for use in lithium-ion batteries and hydrogen peroxide sensors, therefore adding to energy storage and environmental monitoring technologies [41]. The many applications highlight the importance of ferrites in modern technology.

The capacity to manipulate the characteristics of ferrite materials during synthesis is critical for adapting them for specific purposes. The preparation method has a substantial influence on ferrites' structural, dielectric, and magnetic properties [17]. Different techniques may result in variations in particle composition, size, and shape, affecting the material's overall performance. As a result of size dependency, rigorous synthesis methodology selection and optimization are important for attaining the desired characteristics in the final product [40,42]. Researchers may fine-tune the properties of ferrites to meet the requirements of a variety of applications, ranging from high-frequency electrical components to biological imaging agents, by properly manipulating the synthesis parameters. Furthermore, choosing proper parameters in the synthesis process might boost ferrites are widely used, assuring their efficacy and dependability in several technical domains [42].

There are several ways for producing ferrite NPs, each with its own advantages and disadvantages. Some examples of these techniques include sol-gel, hydrothermal, co-precipitation, and thermal breakdown etc. as shown in Fig 9 below. The co-precipitation procedure is a simple and cost-effective way to generate large volumes of NPs, but the sol-gel method allows for precise control over the composition and homogeneity of the final product. Thermal breakdown can give NPs with restricted size distributions, whereas hydrothermal synthesis allows for the creation of extremely crystalline materials under moderate circumstances [43]. Furthermore, the methods of sol-gel auto-combustion and co-precipitation are frequently used to produce nanocrystalline cobalt ferrite powder, allowing a variety of approaches for producing this critical magnetic material [44]. The citrate precursor approach, along with sol-gel auto combustion and hydrothermal spray pyrolysis, are innovative synthesis methods for cobalt ferrite production, providing more choices for customizing the characteristics of the resultant NPs [45]. Understanding the principles and variations of these synthesis methods is critical for developing and manufacturing ferrites with specific properties for specific applications.

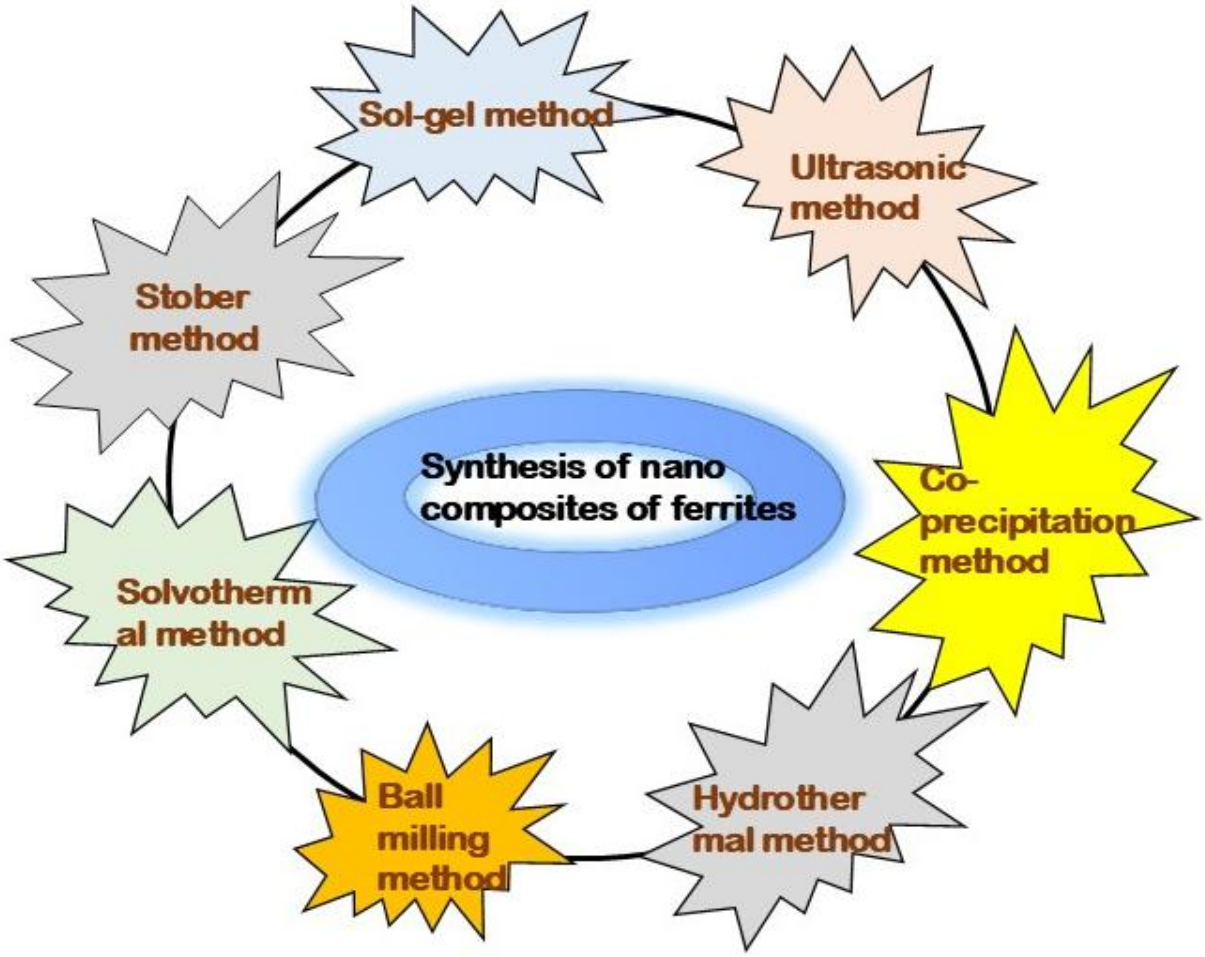


Fig. 9: Synthesis Method for Nanocomposite of ferrite.

5.1 Sol-Gel Method: Principles and Variations

The sol-gel process, a versatile method for creating ferrite materials, provides precise control over particle size, homogeneity, and content. The sol-gel technique is based on the use of metal nitrates as precursors and citrate as fuel, which react in solution to form a gel [46]. Shortly thereafter, this gel is heated, causing ferrite NPs to form. The sol-gel approach guarantees uniformity and excellent purity in the produced materials, making it appropriate for applications requiring high-quality ferrites [47]. Furthermore, the sol-gel approach can minimize process steps and the time spent creating powder, simplifying a production process and increasing efficiency [48]. By carefully controlling the amounts of precursors and reaction conditions, researchers can alter the properties of the produced ferrites to satisfy specific application needs. There are several sol-gel techniques, each with its own advantages and suitability for specific ferrite formation. Highly exchange-coupled nanosized ferrites are produced using the citrate sol-gel combustion process [49] which are ideal for applications needing increased magnetic characteristics. In this procedure, citrate is used as a complexing agent to promote the production of a homogenous gel, followed by burning to eliminate organic components and crystallize the ferrite phase [50]. One approach for synthesizing single-phase $NiFe_2O_4$ and $CoFe_2O_4$ ferrites is the sol-gel self-propagating combustion process, which provides a straightforward way to acquire these key magnetic materials in their pure form [51].

Furthermore, citrate-gel auto combustion is employed to create manganese-doped cobalt nanoferrites, allowing individual dopants to be included to change the electrical and magnetic properties of the final ferrites [52]. Researchers may use Sol-gel's spectrum of approaches to choose the best way for synthesizing ferrites with certain qualities. When compared to other synthesis processes, the sol-gel methodology offers several advantages. It makes it possible to have precise stoichiometric control, ensuring that the final product has the desired chemical composition [48]. Additionally, Smaller particle sizes can be produced as tiny powders using the sol-gel technique, and this is essential for uses where increased reactivity and surface area are required [45]. However, one disadvantage of the Sol-gel approach is the agglomeration of particles, which can limit the performance. Various strategies, such as the use of capping agents and optimized drying procedures, can be employed to minimize agglomeration and improve the overall quality of the synthesized ferrites. Despite this challenge, High-quality ferrite materials with specific characteristics may still be produced using the sol-gel process.

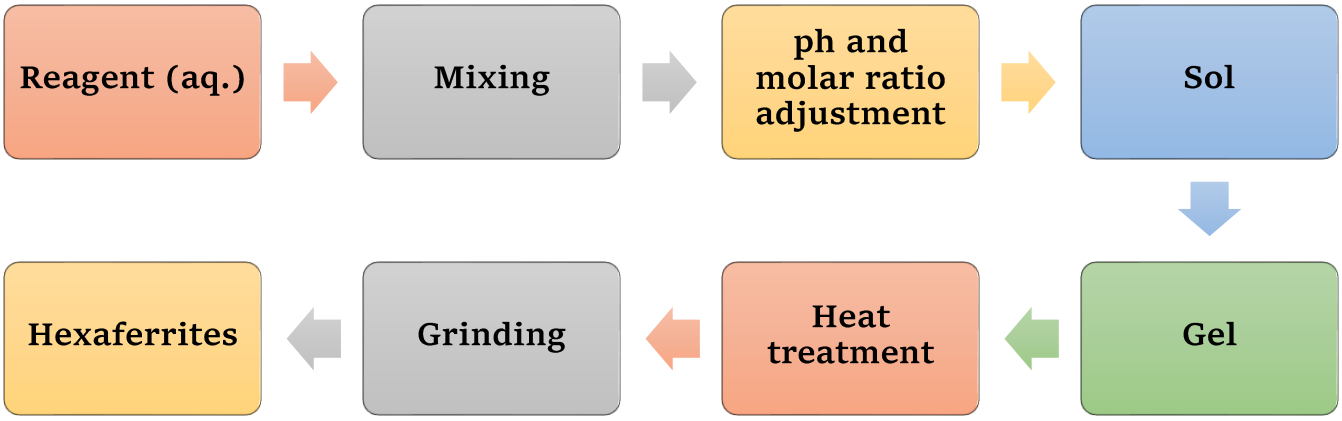


Fig. 10: Basic steps for the sol-gel method [53]

5.2 Co-precipitation Method

Ferrite NPs are frequently synthesized via the co-precipitation approach because of their ease of use, affordability, and capacity to provide comparatively tiny NP sizes. The fundamental principle of the co-precipitation, a precipitating agent, such as a base, is added to a solution to cause many metal ions to precipitate out of it at once [43]. This process results in the formation of a solid phase containing the desired metal ions in a controlled stoichiometry [54]. Co-precipitation is a well-known method for synthesizing NPs with relatively tiny sizes, making it ideal for applications requiring a large surface area and quantum confinement effects [55]. Furthermore, co-precipitation with citrate is employed to produce magnetic NPs of mixed calcium/manganese ferrite, highlighting the method's adaptability in creating complex ferrite materials with customized characteristics [56]. By carefully controlling the reaction conditions and precursor concentrations, researchers may modify the particle size, shape, and composition of the resulting ferrites.

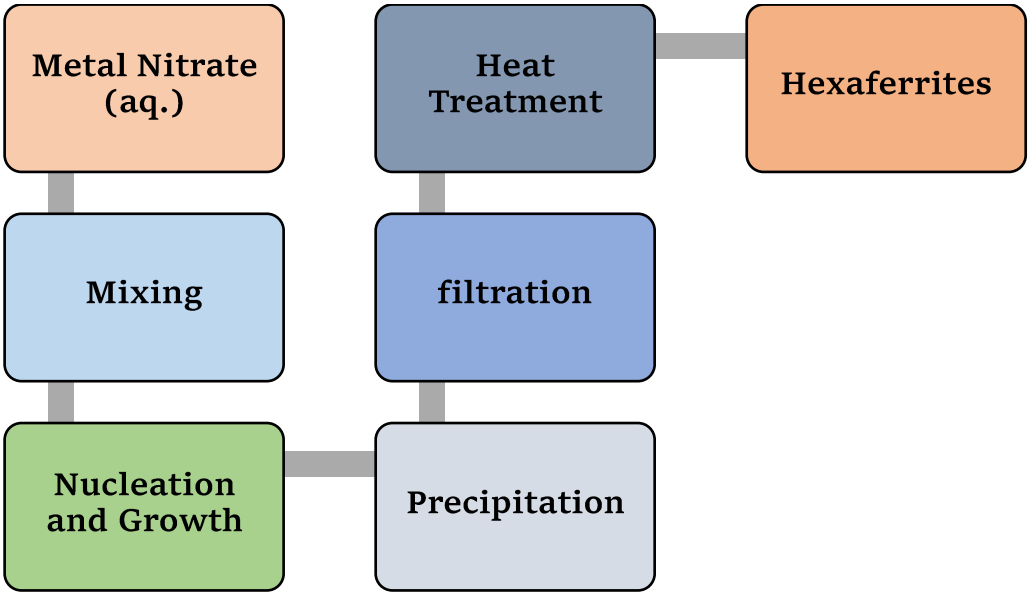


Fig. 11: The basic steps for producing HF utilizing the co-precipitation process [53]

Several factors impact the shape and size of ferrites formed by co-precipitation, as shown in Fig 11. Longer reaction periods tend to result in bigger particles due to Ostwald ripening, which influences the co-precipitation particle size. Capping agents minimize aggregation in co-precipitation by stabilizing the NPs and preventing them from clumping. These capping agents, such as surfactants or polymers, adsorb onto the NPs' surfaces, forming a steric or electrostatic barrier that prevents agglomeration [57]. Higher annealing temperatures promote grain growth and increase the size of the crystallites within the NPs [58]. In order to generate ferrites with the correct particle size and shape, these characteristics must be carefully controlled. It is a relatively easy and safe fabrication method that requires little equipment and expertise. The co-precipitation process yields NPs with relatively tiny sizes, which is useful for applications that need a large surface area and quantum confinement effects. However, co-precipitation can cause aggregation in the absence of effective capping agents, reducing the material's performance and effective surface area [55]. To address this issue, researchers frequently use capping agents or surface modification methods to increase the stability or dispersibility of synthetic ferrite NPs. Despite this restriction, co-precipitation remains a common technique of creating ferrite materials due to their low cost and ease of usage.

5.3 Citrate Method: Mechanism and Synthesis of Ferrites

The citrate technique, which is commonly used to manufacture ferrite materials as shown in fig 12 below, allows for precise control over the end product's chemical composition and homogeneity. The citrate method's detailed mechanism includes the use of metal nitrates as precursors and citrate as fuel, which react in solution to form a complex [46]. In the citrate technique, citric acid acts as a complexing agent, attaching to metal ions and avoiding early precipitation [45]. When heated, the citrate undergoes a combustion process, releasing energy and driving the production of the ferrite phase. Citrate can also stabilize NPs in co-precipitation, preventing agglomeration and promoting the formation of well-dispersed particles [56]. The functionalities of the synthesized ferrites can be modified by researchers to satisfy particular application needs by carefully regulating the reaction conditions and precursor ratios.

The citrate method has been used effectively to synthesize a large number of ferrites with particular properties. Several metal ions can be added to the ferrite lattice by employing the citrate gel approach to create nanostructured ferrites with specific compositions [59] . The citrate precursor approach is employed

to create $Mn_{0.2}Ni_{0.2}Zn_{0.6}Fe_2O_4$ ferrite NPs, proving its capacity to make complex ferrite materials with regulated stoichiometry [60]. Furthermore, the citrate sol-gel manufacturing technique is used for fine powders of doped BaF, allowing for the incorporation of additives that alter the final ferrites' electrical and magnetic properties [61]. The citrate method's versatility makes it a useful tool for researchers looking to develop and synthesize ferrites with specified properties for a variety of applications.

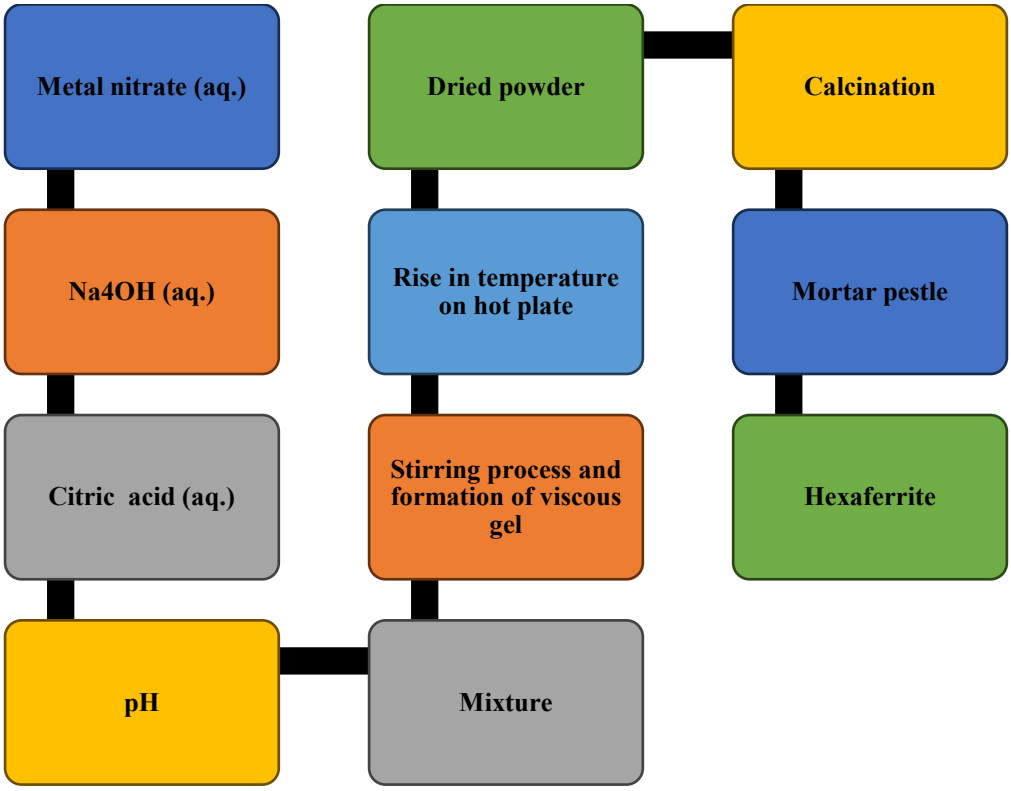


Fig 12: Procedures for HF synthesis using citrate.

As a synthesis technique, the citrate method has both advantages and disadvantages. It ensures uniformity and improved properties in the resultant ferrites, which leads to better performance in a variety of applications. The citrate approach enables exact stoichiometric control, guaranteeing that the end product has the correct chemical composition. The citrate approach generates single-phase cubic spinel crystals, which are ideal for many magnetic and electrical applications. However, the citrate method can be extremely complex and time-consuming in contrast to other methods, including co-precipitation. Despite this limitation, the citrate method remains a powerful tool for producing high-quality ferrite materials with tailored properties.

5.4 Hydrothermal method

Materials that are generally insoluble are dissolved and recrystallized using the hydrothermal synthesis technique, which involves a heterogeneous interaction with an aqueous solvent at high pressure and temperature [62]. The hydrothermal approach is a flexible way to manufacture advanced NPs. Due to the high heat and pressures involved in preparation, the word came from earth science. In this process for synthesizing ferrites, a saltwater solution is prepared, and drop by drop, NaOH or KOH is added. The involvement of NaOH or KOH is crucial in the formation of metal nitrate precipitates from the watery mixture. The mixture is stirred to ensure uniformity and then placed in an autoclave (a specialized reactor used to conduct reactions under high temperature and pressure). Thermal treatment is applied to the

solution by heating the autoclave in an oven between 150 and 290°C. After the precipitates are produced, they are filtered, cleaned, and oven-dried.

5.5 Solvothermal method

The synthesis using the solvothermal technique is helpful for creating ferrite materials with enhanced chemical and tangible characteristics that can be used in both industrial and biomedical settings. In the solvothermal process, metal precursors are mixed into a solvent, which can be either aqueous or non-aqueous. To encourage the production of crystals, the resultant mixture is heated in an oven and autoclaved to generate high pressure and temperature. The boiling point of the solvent rises due to its vapor pressure. The crystals are then cleaned and dried. This method is known as the solvothermal technique.

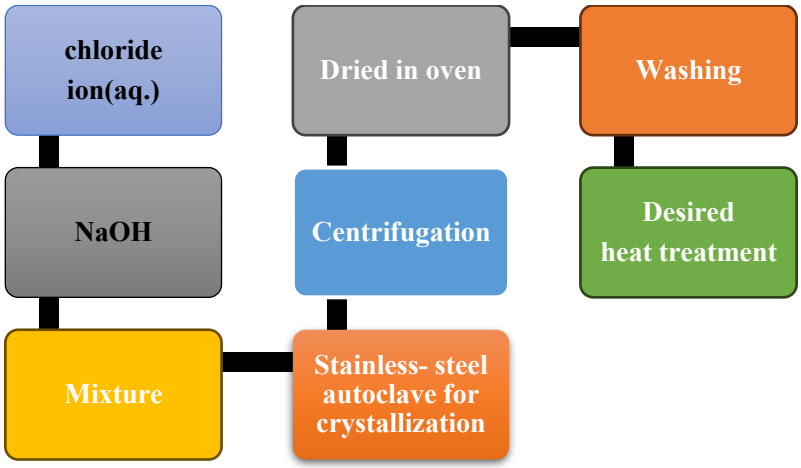


Fig.13: Procedures for the solvothermal technique of HF preparation

5.6 Thermal decomposition method

A thermal breakdown process (shown in Fig 14) was used to make $Ni_{1-x}Zn_xFe_2O_4$ (x = 0.5, 0.6, 0.7) NPs. Basic ingredients included nickel (II) acetylacetonate (97%) and zinc acetylacetonate hydrate (95%). Benzyl ether (98%) was employed as a solvent, 1,2-hexadecanediol (90%) as a reducing agent, and oleic acid (90%) and oleyl amine (70%) as surfactants. In accordance with the chemical form of $Ni_{1-x}Zn_xFe_2O_4$ (x = 0.5, 0.6, and 0.7), the precursors of Ni, Zn, and Fe-acetylacetonate were weighed, respectively, and then poured into a 500 mL three-neck flask that was filled with an oleic acid mixture containing 6 mol, heated to 200 °C for an hour, and then heated to 300 °C for an additional hour. Refluxing cooling water and a N_2 environment were used for the technique. To get rid of any last bits of organic material from the ferrite particles, the solution was centrifuged for 30 minutes at 4000 rpm after the reaction was finished and allowed to cool to room temperature. It was then repeatedly washed with ethanol and hexane. Fatty acids like oleic acid and oleyl amine were dissolved in hexane. Final steps were collecting and drying $Ni_{1-x}Zn_xFe_2O_4$ (x = 0.5, 0.6, 0.7) NPs at 100 °C for 24 hours using 20 mL of benzyl ether, 1,2-hexadecanediol (HDD), and mmol oleyl amine.

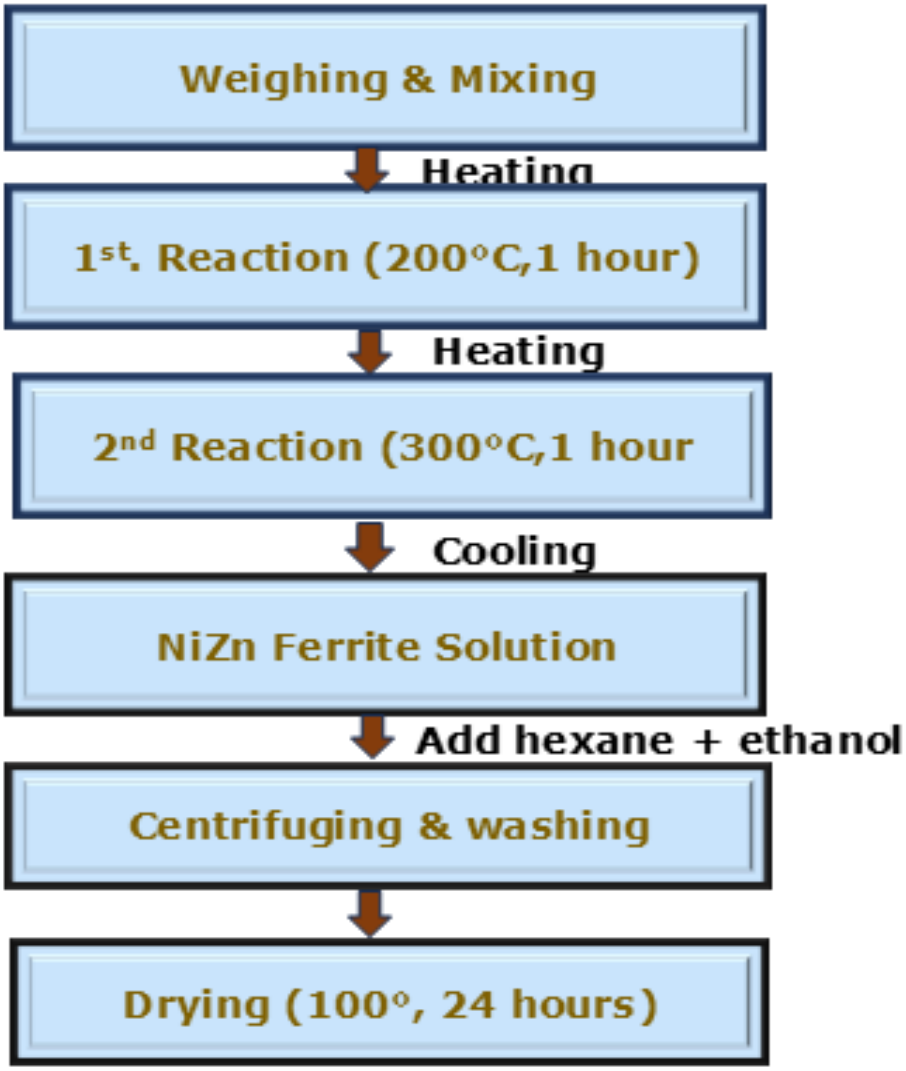


Fig.14: Steps for the preparation of hexaferrites by thermal decomposition method [62]

5.7 Auto Combustion Method

The most common acronym for the auto-combustion process is the modified sol-gel citrate method as shown in Fig 15. The necessary metal salts (oxidizer) and organic complexant (reductant) are added to a solution made from water, xerogel undergoes a self-sustaining exothermic anionic redox reaction caused by heat. In order to provide the oxidizer/reductant relation equal to 1, proportions between complexants and salts are often computed based on the valences of the reactive components. Since the nitrate salts constitute a water-soluble source of NO_3 oxidants at low temperatures, they are preferred as precursors. In certain instances, complexants and metal nitrates are combined immediately by vigorous heating and stirring not using water. The hygroscopic nature of metal nitrates allows them to easily absorb moisture and form a slurry.

The flash-combustion method is the name given to this kind of auto-combustion sol-gel.

Ferrite NPs are created when a huge volume of gasses is rapidly evaluated and a significant mass loss occurs during the xerogel combustion. The development of gases restricts agglomeration. Crystalline ferrite is directly converted from xerogel during combustion, which is surely caused by the heat generated by the exothermic process. The temperature of the flame can fluctuate between 600°C and 1350°C during

burning. The processing process flow chart is displayed in Fig. 15. The sol-gel auto-combustion method offers several advantages, including excellent chemical homogeneity (mixing of cations with the desired composition at the molecular level), high product purity and crystallinity, a fine and narrow particle size distribution, straightforward stoichiometry control, the ease of incorporating dopants into the final product, reduced processing time, minimal external energy consumption (initiating at low temperatures), and the elimination of multiple processing steps.

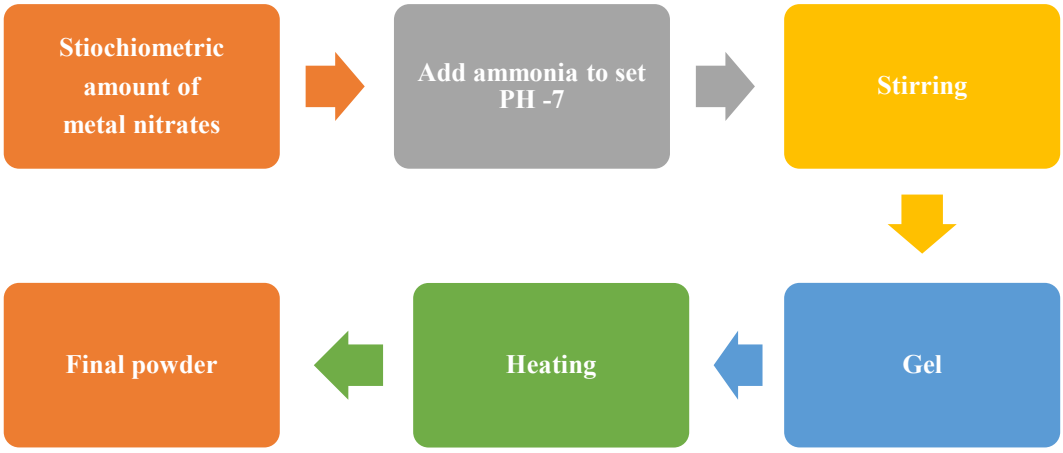


Fig.15: The fundamental stages involved in producing HF using the auto combustion technique.

5.8 Mechanical Milling

NPs are often produced by grinding on a machine in glass mills, planetary ball mills, or high-energy shakers. The procedure is an example of a top-down method for producing ferrite NPs. The capacity to enlarge to enormous tons of material for a variety of purposes is this method's greatest advantage; nevertheless, one of the biggest problems with milling is that it can contaminate NPs. $CoFe_2O_4$, $CuFe_2O_4$, and $NiFe_2O_4$ are among the several ferrite NPs that have been synthesized via mechanical milling. The milling process is an easy and affordable technique to create ferrite NPs[13].

5.9 Green synthesis

Green synthesis methods have gained significant popularity due to their simplicity, cost-effectiveness, high stability, reduced time consumption, eco-friendliness, and non-toxic by-products, making them easily scalable for large-scale synthesis. In the green synthesis approach, hazardous chemicals are replaced with safer alternatives. The production of ferrite NPs frequently involves the use of organic or plant-based components. However, there may be some disadvantages, such as uncertainties with recycling, reuse, and regeneration; bioaccumulation; and instability in harsh conditions. Kagdi et al. Different amounts of ginger (Zingiber officinale) root extract were utilized to synthesize X-type Barium-Zinc HF, having the chemical formula $Ba_2Zn_2Fe_{28}O_{46}$. The powders were synthesized through a combustion treatment process, initially pre-heated at 550 °C for 4 hours using ginger as fuel, then subjected to final heating at 900°C for 5 hours, followed by natural cooling to room temperature to yield $Ba_2Zn_2Fe_{28}O_{46}$ HFs powder. The phase composition of the heated powder samples was examined through X-ray diffraction (XRD), showing the development of a blend of X-type and hematite (α-Fe_2O_3). At 900 °C, X-ferrite formation reached 82.6% using 52.5 g of ginger root extract. Dielectric analysis of the prepared samples reveals phenomena that depend on frequency. All samples were hard magnets, exhibiting H_c values ranging from 262.2 to 318.3 kA m^{-1}, and squareness ratios exceeding 0.5. The sample made with 52.5 g of ginger root extract shows

the highest saturation magnetisation value (MS = 33.87 Am^2 kg^{-1}) when compared to the other samples prepared. Thus, ginger has been demonstrated to be an effective natural plant extract for reducing fuel in the low-temperature synthesis of X-ferrites. The sample made with 35 g of ginger root extract exhibits a wide loss tangent resonance peak within the 10 kHz to 100 kHz range, whereas the other samples display loss tangent resonance peaks in the 300 kHz to 2 MHz frequency range.

6. Application of hard ferrite in PMs for EVs and Memory devices

6.1 Hard ferrite for PMs

The ferrimagnetic oxides known as hard ferrites, or hexaferrites, have a hexagonal magneto-plumbite-type crystal structure

The M-type HFs materials exhibit an intense uniaxial anisotropy of magneto-crystalline materials, which is the primary explanation for their high H_c, i.e., resistance to demagnetization [30]. HF finds extensive use in numerous PM applications due to their cost-effectiveness, availability, and chemical stability. Although their energy output is less than that of rare-earth magnets, making them appropriate for uses where top performance is not essential. However, the material's magnetic characteristics may be improved to the point that it may be utilised as PM magnets in high-power applications such as EVs after doping it with an appropriate element. This may be achieved by making a few alterations to the hexagonal ferrites' crystal structure, such as decreasing their size at the nanoscale, altering their morphology, substituting divalent and trivalent metal cations to increase their magnetism, and many other adjustments [13].

The structure of magneto plumbite with $P6_3$ space geometry, known as $PbFe_{12}O_{19}$, serves as the basis for the hexagonal ferrites that age to a family of hard ferrites. A kind of hexagonal ferrite, M-ferrite, is composed of one S block and one R block. The unit cell formula SRS*R* is provided by the mirror block R, R*, where * denotes the 90˚ rotation of the specified block around the c-axis. The mirror plane, where the S and R blocks are 180˚ rotated around the c-axis, is the plane that includes the barium atom. Blocks overlap with layers that are packed hexagonally and cubically. It also emerged that BaM ferrite, which is composed of stacking blocks that resemble spinel, and massive scale studies of M-type ferrite, such as BaFe12-xAxO19, have been executed. This has been studied to enhance the fundamentals of BaM ferrite's magnetic properties [13].

Based on the research, the lattice parameters of BaM , SrM and PbM varies with some values. See table below:

Lattice parameters	BaM	SrM	PbM
c	$23.17A^0$	$23.03A^0$	$23.02A^0$
a	$5.89A^0$	$5.86A^0$	$5.88A^0$

The specific features of hard ferrites' magnetic fields are established by both intrinsic and extrinsic factors. Intrinsic details are innate to the crystal structure of the substance and chemical composition, including Magneto crystalline anisotropy, Curie temperature, and saturation magnetization [17]. Extrinsic properties, on the other hand, are related to the microstructure of the material, such as grain size, shape, orientation, and density. Both sets of properties play crucial roles in determining the overall performance of HF in various applications. This may be achieved by making a few alterations to the hexagonal ferrites' crystal structure, such as decreasing their size at the nanoscale, altering their morphology, substituting divalent and trivalent metal cations to increase their magnetism, and many other adjustments.

(a) Magnetic material for PMs

Long before the phrase "materials science" was coined, PMs were the focus of materials research. The

ancient Greeks were aware of magnetite (Fe_3O_4), a naturally occurring lodestone. From the year 1200 to the end of the 1800s, carbon steels were the only material utilized to make PMs; they are occasionally still used today. The most important PMs sold in stores, as well as the first magnet made of carbon steel for real-world applications. These days, PMs are crucial enabling technologies utilized in a variety of sectors and applications, including those in transportation, industry, consumer electronics, residential and commercial settings, military, IT/PC, wind energy, and medicine.
Here schematic representation of the magnetic material used in PMs:

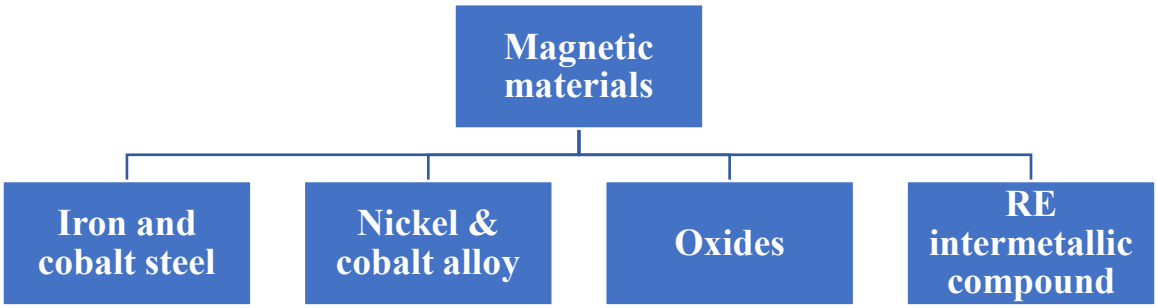


Fig.16: four types of magnetic material used in PMs

(a) Iron and cobalt steel

By the end of the 1800s, tungsten steels made of iron (up to 6% W) had been developed. Cobalt steels were found to be PMs in Japan by 1917. Although they typically utilize 35% Co, they may include up to 40% Co . These steels may be hot worked and machined when annealed. Steel undergoes heat treatment in the austenite zone and quenching to produce martensite in order to achieve H_c. The attendant attraction cannot be machined and is fragile.

(b) Nickel and cobalt alloy

Regard less of whether they include Co or are isotropic or anisotropic, The Al–Ni–Fe and Al–Ni–Co–Fe magnets were developed by Mishima in 1931. These magnets are commonly referred to as "Alnicos." Both casting and sintering can be used to create them. The range of cobalt concentration is 12–30%. The Hc rises as the Co content does. The variation known as "Alnico 8" has a composition of 34 Co, 5 Ti, 5 Cu, 7 Al, 14 Ni, and balance Fe (wt %) and is produced through field annealing and hardening of precipitation with an energy product of up to 8 MG Oe. Although ferrites and RE magnets have mostly supplanted Alnicos, some are still made.

© Oxides

Ba-HF ($BaFe_{12}O_{19}$) is used in permanent adhesives and its derivatives are the most significant oxide. These materials, which were uncovered in 1950 at the Philips laboratories, completely changed how PMs are used in daily life. The literature provides an overview of ferrite magnets (e.g. Mc Currie 1994). Regarding volume, ferrite magnets are produced in greater quantities than any other kind of magnet; but in the case of overall value, the producing process of PMs based on RE is gradually catching up to ferrites.

(d) RE intermetallic compound

A potentially good PM material would be an intermetallic compound with a strong easy-axis anisotropy and a moderately high saturation magnetization and Curie temperature value. Since the 1950s, the USA has conducted systematic research into RE alloys and compounds to determine the characteristics that are relevant to their application in PMs. Major players in these investigations that led to the discovery of the

significant crystals ,the authors of the YCo5 crystal anisotropy were Strnat (Wright Patterson Air Force Base, Dayton), Wallace (University of Pittsburgh), Nesbitt, Wernick, and Geller (Bell Labs) & Hubbard and Adams (Naval Research Laboratory) [63]

(e) Commercially available PM:

There are five types of commercially available PMs as shown in Fig 17.

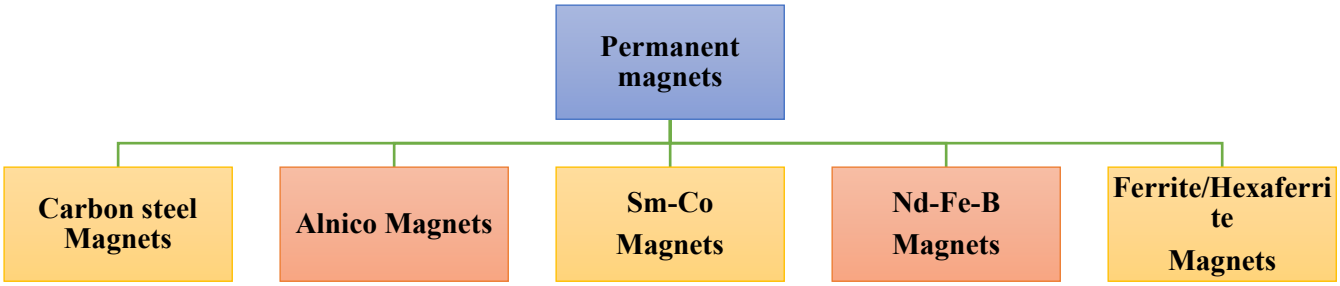


Fig.17: Types of PMs

(f) Carbon Steel Magnets

The M_s of magnetite is higher than that of carbon steel magnets. A tiny reversible field can demagnetize carbon steel due to its poor H_c. By 1885, steel with 5% tungsten was being made and used for magnets after it was discovered that alloying steel with other metals improved its magnetic properties after 1880. It has been said that carbon steel with 30–40% cobalt, tungsten, and chromium has the greatest H_c of any magnetic material (230 Oe) and an enhanced energy product of up to 1 MGOe. However, compared to those made ten years later, steel magnets had noticeably worse magnetic characteristics. The finest steel magnets are costly because of the large proportion of costly cobalt elements. As a result, these magnets were no longer produced commercially and were swapped out for more contemporary, high-performance models.

(g) Alnico Magnets

Mishima created the PMic alloy alnico in 1931. Originally composed of iron, nickel, and aluminium, in order to increase the BH_{max} and H_c, cobalt was then added. In addition to various alloying elements like Al, Ti, and Cu, the primary constituents of alnico, a permanent magnetic substance, are Fe, Co, and Ni. In applications like traction motors, Alnico alloys can be used in place of rare-earth PMs owing to their exceptional thermal stability (up to 400 °C). Because of its high-temperature stability, Guitar pickups, MRI machines, and electric motors and generators all require alnico alloys, and navigational devices in aircraft and aviation. Alnico alloys, ferrites, and magnets that incorporate REE, such as NdFeB and SmCo, make up the majority of PMs. PMs are widely used in electric motors, wind turbines, generators, and

alternators to convert electrical energy into mechanical energy and vice versa. PM materials have high H_c ranging from 0.5 to 35 kOe, a M_r of 0.7–1.5 T, and a maximum energy product (BH_{max}) of 0.75–54.04 MGOe. PMs are frequently employed to transform electrical energy into mechanical energy and vice versa in electric motors, wind turbines, generators, and alternators [13].

(h) Sm-Co Magnets

Due to their magnetic qualities, particularly their magnetic energy density and the natural coercive force, Sm-Co-based magnets outperformed commercially available hard ferrite and Alnico magnets and saw a relatively quick commercial development from the late 1960s until the late 1970s. Powder metallurgy is used to create these novel PM classes, $SmCo_5$ and Sm_2 (Co, Fe, Cu, Zr)$_{17}$. In contrast to alternative PM classes, these magnets have superior magnetic qualities at high temperatures, outstanding corrosion resistance, and exceptional thermal stability. Owing to these characteristics, Sm-Co magnets is the ideal option for an extensive variety of demanding uses such as, electronic countermeasures, accelerometers and gyroscopes, high-speed motors and generators, medical devices, and traveling wave tubes for space exploration and satellite communication [64].

(i)Nd-Fe-B Magnets

High-performance PMs that are built on $Nd_2Fe_{14}B$ are made using a variety of production methods and compositions. The intricate, multiphase microstructure of the magnets is influenced by the composition and the manufacturing method, which affects phase distribution, alignment, and grain size. The HDDR (Hydrogen decrepitation deabsorbation recombination) technique, mechanical alloying, and melt spinning are used to produce grain sizes in the 10–500 nm range. Grain diameters in hot-worked and sintered magnets are more than 1 μm In small-grained magnets, exchange coupling reduces the coercive field, but the dipolar interactions between misaligned grains are more noticeable. How advanced (Nd,S1)–(Fe,S2)–B:(M1,M2) magnets' microstructure, Hc, and corrosion resistance are affected by substituent and dopant components has been investigated using transmission electron microscopy. Particularly in large-grained magnets, corrosion resistance is increased by substituting stages that are secondary created obeying M1 and M2 type doping elements for the Nd-rich intergranular phase. The energy product and M_r are decreased by secondary, nonmagnetic phases. The computer simulation of the interaction between H_c and microstructure has received particular attention in addition to the microstructure's characterisation. Both the magnetization models and the experimental measurements accord well with the reversal process based on the actual microstructure.

PMs based on NdFeB have a multiphase, intricate architecture. The ternary phase diagram indicates that there are at least three equilibrium phases [65]: The hard magnetic $Nd_2Fe_{14}B$ phase, the boride phase $Nd^{1+e}Fe_4B_4$, and the low melting Nd-rich phase (n).. Certain substituent elements significantly alter intrinsic features, including Magneto crystalline anisotropy, the Curie temperature, and spontaneous polarization by replacing the Fe atoms with S_2 , Co, Ni, and Cr, and the Nd atoms with S_1, Dy, Tb, in the hard magnetic phase, respectively. The H_c of the magnets is weakened by the generation of soft magnetic Nd-(Fe, S2) intermetallic phases, which involves the Laves-type (NdFe, S2)$_2$-phase [66].

(j) Hexaferrite magnets

Humans have been using PMs for thousands of years, first in the form of lodestone and then in the form of magnetized steel. Their practical application was restricted to the compass for most of history, and for most people, they continued to be nothing more than a sort of magic trick. The widespread usage of magnets didn't start until the Industrial Revolution. These days, a lot of technologies employ materials for PMs, particularly in sensors and information storage. Furthermore, they are transducers that connect

electrical to mechanical and mechanical to electrical. Thanks to advancements in material science and concurrent technological development, materials have been produced since the beginning of the twentieth century with the express purpose of improving the ancient magnetic materials. These metallic alloys led to the discovery of Mishima's work on the Alnico family in the 1930s, the development of Phillips' hard ferrites through the 1950s, and the development of Rare-earth powerful magnets SmCo and NdFeB in the 1970s and 1980s, respectively. The variation of the properties required for a hard magnet, like the magnetic anisotropy, has increased in tandem with this growth.

Hard ferrites, such as the M-type HF, i.e., BaF, and SrF, and similar materials, now dominate the ferrite magnet industry. Ferrites have modest M_s or magnetization induction $B_s = \mu_0 M_s$, specific saturation (σ_s), and M_r (M_r induction, $B_r = \mu_0 M_r$), but they have comparatively substantial H_c up to 380 kA m^{-1}. The magnetic hardness, or κ, is a valuable measure to empirically demonstrate a material's eligibility to produce a compact PM without forming limitations. The definition of this is given by the ratio $\kappa = (K_1/\mu_0 M_s^2)^{1/2}$, the magnetostatic energy to anisotropy, K_1, and it is thought that $\kappa > 1$ is the threshold for a material to be considered hard. Despite their moderate anisotropy and relatively low M_s, M-type HF is often employed to create PMs because of their hardness, which is more than 1 (for instance, for BaF $\kappa = 1.34$). The Hitachi Metals NMF-15 series, the best ferrite magnets available, can achieve maximum M_r induction values of 480 mT. Their figure of merit for magnet strength, the maximal energy product (BH_{max}), is 44 kJ m^{-3}. In contrast to rare-earth-based materials like Nd–Fe–B, which usually exhibit M_r of 1.3 T, H_c of 1500 kA m^{-1} ($\mu_0 H_c = 1.85$ T), and energy products of 350 kJ m^{-3}.

Ferrites do, however, have a few significant benefits. The primary one is unquestionably the accessibility and regarding the relatively cheapness of raw materials in a powdery form, which cost around 1.5 \$ kg^{-1}, whereas powdered NdFeB costs about 60 \$ kg^{-1}.They are also exceptionally chemically stable and electrically resistant. Since increasing the amount of magnetic material may compensate for the low flux density, ferrite magnets are commonly used in mass applications where significant energy products are not required or where increasing the device's weight is not a concern. The result of their low eddy current losses they include electromagnets, transformers, and inductors. Due to those features, ferrite magnets become one of the most often used PMs in terms of weight.

6.1.1 The possibilities & difficulties of enhancing ferrite magnets

Crucial raw resources, such as rare-earth elements, cause price volatility, supply risk, and environmental problems. These factors have a direct impact on the PM value chain which is why significant efforts are being made to lessen our reliance on them. Enhancing the potential to recycle gadgets and materials made of rare earth elements, formulating competitive innovations devoid of rare earth elements, and identifying substitute magnets for NdFeB and SmCo magnets are some of the tactics. Ferrites are an intriguing alternative as they are the most often used magnet by volume worldwide. However, ferrites' magnetic characteristics must be enhanced to allow for a wider substitution in more applications. The market for PMs is expected to be driven by the substitution of ferrites in essential applications, which will raise the need for NdFeB in the coming years. This replacement is, in fact, typically possible in applications that require magnets with modest $(BH)_{max}$ (50–200 kJ m^{-3}). This category includes generators used in wind turbines and automobiles, and the creation of rival devices based on superior or upgraded ferrites may need widespread substitution. The significance of ferrite-based magnets is being reemphasized in light of this need.

HFs in sintered ceramics have a $(BH)_{max}$ value of around 40 kJ m^{-3}. For almost 40 years, the majority of the H_c values that are utilized to estimate $(BH)_{max}$ have been frozen. Both sintered and bonded commercial

magnets have coercive fields that are comparable to the Mr induction and close to the saturation induction (0.4 T), given that the BaF and SrF's substantial magnetic anisotropy fields, 1.7 T and 1.8 T, respectively, are significantly bigger than those of H_c and M_s. In the present scenario, the $(BH)_{max}$ is almost the maximum value that might have been accomplished. Therefore, improving the saturation induction is necessary for the first method to raise the $(BH)_{max}$.

For PMs, on the other hand, it should be taken into account that H_c should be greater than $N_{eff}M_s$ in order to prevent demagnetization, where N_{eff} is the demagnetizing factor because of the magnet's form. To maintain $H_c > N_{eff}$ Ms, a second goal is to strengthen the coercive field. A further increase in the magnetic anisotropy, K_1, is necessary to achieve the goals of enhancing both H_c and M_s by upgrading a single-phase material since the H_c is proportional to the anisotropy field and, thus, to K_1/μ_0 Ms. However, it is important to consider that altering the magnetic structure may result in other modifications to the ceramics' characteristics. The first is the shift in the Curie temperature, or T_C, and consequently the exchange interactions. The magnetization may decrease more quickly than in typical ceramics in the specific instance of the Curie temperature dropping. This may have an adverse effect on the application of magnets in high-temperature settings.

Another factor to take into account is that the negative thermal coefficient of HFs makes the coercive field increase with temperature. This makes ferrite magnets often perform better up to 100 °C than at room temperature. The temperature dependence of H_C depends on the relative temperature dependences of both K_1 and M_S, which should vary with the doping due to the change of the T_C. Any changes to each component might thus negatively affect the resulting useful temperature range. In light of the present need for improved ferrite magnets, we examine here the most promising approaches and current findings to enhance the functionality of HFs materials for PM applications. We outline three primary avenues for further advancement. First, we look at how modifying the size and structure of HF NPs might enhance their commercial counterparts' magnetic qualities [67].

The three main themes that are explored in the second section are the improvement of the well-known La–Co-doped BaF system, doping modifications to increase the M_s, and doping modifications to increase the H_c. We examine first exchange-linked composites with oxide or metal components in the third part. We address the potential for utilizing internal magnetostatic interactions to enhance the characteristics of composites and offer our thoughts on the encouraging outcomes of highly coherent magnetite-HF platelets. Lastly, the findings and potential applications of ferrite magnets are discussed [68].

6.1.2 Factors that enhance hard ferrites' performance for use in PM applications in EVs:

(a) Reduction of size

Of them, reducing the grain size to the nanoscale is widely acknowledged as a practical way to increase a magnetic material's Hc. Alnico alloys, one of the greatest PMs, are in fact nanocomposite materials. Alnico alloys, which are still important in the PM market 90 years after they were first introduced, are made up of elongated FeCo-rich ferromagnetic nanograins scattered throughout a weakly magnetic Al–Ni matrix. By applying an external magnetic field during the annealing process, the material's BH_{max} may be further increased. The reversal of magnetization in a bulk ferro (ferri)-magnetic material can happen via a variety of processes, including domain wall pinning and the nucleation and propagation of reverse domains [68]. However, on squeezing the volume of the material, a critical size is reached below which the formation of domain walls is no longer energetically favored, and a single domain (SD) spin configuration is attained. The magnetic behavior of the SD particle can then be described by a giant magnetic moment $\mu = M_S V$, where V is the volume, arising from the combination of the individual atomic spins, which reverses its

orientation through the coherent rotation of the single spins. For a given material, the critical diameter, d_C, for the SD spin configuration state depends on the competition between three energy terms, magnetostatic energy, magnetic anisotropy constant, K, and exchange energy, A.

For a spherical nanocrystal, d_c, is expressed as [69]:

$d_c = (18E_\sigma)/(\mu_0 Ms^2) = (36[AK]^{1/2}) / (\mu_0 Ms^2)$

where $E\sigma = 2(AK)^{1/2}$ is a domain's surface energy and μ_0 is its vacuum permeability. For the majority of magnetic materials, typical d_c values vary from a few tens to many hundreds of nm [70]. Although larger values up to 1 μm have frequently been recorded, theoretical and experimental estimations for Ba-ferrite indicate that d_c is around 500 nm [71] [72]. For SrF, critical diameters as small as 1.5 μm have also been recorded [73][74] and colleagues calculated the activation volume of a set of BaF particles ranging in size from 65 nm to the micrometric range, or the size of the nucleus that causes magnetization to reverse. When the particle size dropped below 800 nm, the coercive field increased from 200 kA m^{-1} to 320 kA m^{-1}, and the activation size dropped from 40 nm to 25 nm during the course of the series. The authors concluded that coherent rotation is the fundamental reversal process for the smaller particles, whereas domain wall propagation is the reversal mechanism in the particles larger than 800 nm [75].

There are several non-uniform reversal modes, such as curling and buckling, when implausible coherent reversal occurs, and the exchange energy does not stay constant during the transition from the multidomain (MD) to the SD state (As shown in figure 18 given below.) [76] [77]. For instance, Chan et al. used magnetic force microscopy to measure the switching field of a set of isolated BaF NPs. They discovered that the Stoner–Wohlfarth model only applied to average sizes up to 50 nm; as the size increased beyond this point, incoherent reversal modes caused the switching field to decrease [78]. Furthermore, a study using electron holography to examine the magnetic domain structure of isolated BaF particles made by heating a mixture of $BaO \cdot Fe_2O_3$ and an additive of Bi_2O_3 to 1100 °C showed that SD and two-domain magnetic states coexisted throughout the entire examined range of 0.1–2 μm [72].

As long as the SD threshold is met, the H_c rises as the grain size decreases due to the size dependency of the reversal process, as graphically seen in the Fig 18. The NPs really grow unstable against thermal demagnetization as their size decreases, eventually achieving the SPM state and total magnetic irreversibility. The form and crystal quality (defects and impurities) of the grains determine the threshold size below which superparamagnetism may be detected for a specific measurement duration. It is often believed that SPM relaxation takes over for BaF and SrF at sizes smaller than 40–60 nm [79] [80]. The shelf life needed for a PM (the loss of magnetism must be less than 5% over 100 years) is far longer than these restrictions, which are frequently related to the time scale features of laboratory experiments (usually between 102 and 104 s).

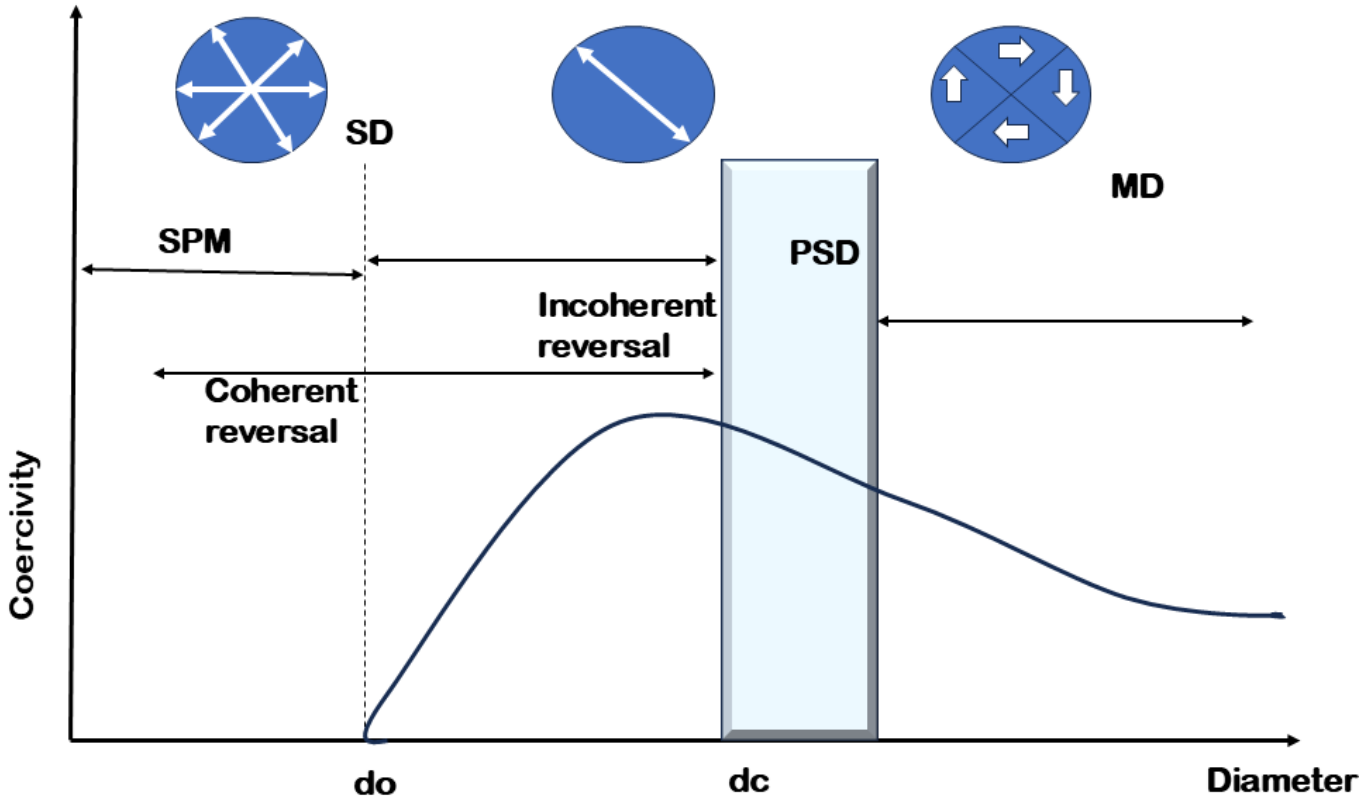


Fig.18: Scheme of the room temperature variation of Hc with the grain size from SPM to SD & MD states.

PSD denotes the pseudo-single domain region (PSD), while the light grey zone indicates the size range where incoherent reversal processes might occur [81]

A thorough analysis was conducted on a family of polycrystalline BaF samples generated by a typical solid-state process [82] neatly corroborated the predicted trend of the H_c with the particle size. By raising the calcination temperature from 1000 °C to 1400 °C, the particle size was adjusted between 500 nm and several microns. As the grain size increased, the coercive field was seen to decrease from 318 kA m^{-1} for the smallest samples to just 100 A m^{-1}. The authors contended that pinning of the magnetization at grain boundaries, whose extent scales with the reciprocal of the size, determines H_c at tiny sizes. On the other hand, they proposed that the H_c originating from nucleation and domain wall pinning is modest in the larger multi-domain grain. In addition to confirming that the crucial single domain size is about 500 nm, our work showed how the size of the grains may readily alter the H_c of BaF.

(a) The consequence of shape:

The coercive field is determined in part by the form of the particles as well as their size. The anisotropy field, H_A, for non-interacting single domain spheroidal particles may be expressed as follows, according to the Stoner–Wohlfarth model: $H_A = H_K + D_N M_S$, where D_N is the demagnetizing term and $H_K = 2K_1/\mu_0 M_S$ is the magnetocrystalline anisotropy. The value of D_N may be positive or negative, depending on whether the easy axis is parallel to or perpendicular to the main axis of the spheroid.

Along the short dimension, M-type ferrites naturally tend to take on a regular hexagonal thin platelet structure with the c-axis, which aligns with the magneto-crystalline easy axis. The development of low-

energy {001} crystallographic faces is correlated with this form. However, depending on the synthesis circumstances, acicular platelets are frequently produced. In this case, the magnetization along the easy axis results in a significant demagnetizing field. $H_A = H_K - D_N M_S$ provides the reduction in magnetic anisotropy caused by the shape contribution. Although D_N is a tensor, it may be thought of as a scalar for simplicity's sake. The diameter (D) to thickness (t) ratio determines the D_N term, which is equal to 1 when $t \geq D$ (as in the case of thin platelets) and falls with D/t to zero for equiaxial morphology (D/t = 1). When $D/t < 1$, H_A rises in relation to H_K and D_N changes sign. However, one benefit of platelet shape is that it makes tiny particles (those smaller than 100 nm) easier to orient mechanically or magnetically. Grain orientation along the c-axis is a key characteristic because it enables the reduced M_r to increase from half the M_s, the value obtained for isotropic magnets made from powders made of SD, randomly oriented particles (0.5 is the theoretical value predicted by the Stoner–Wohlfart model, which corresponds to $(BH)_{max}$ of about 8 kJ m^{-3}), to values near 1. The coercive field is likewise expected to rise with direction according to the Stoner–Wohlfart model; in fact, for oriented particles, H_c corresponds with H_a; however, for non-interacting randomly oriented particles, $H_c = 0.49\ H_a$. Processing from powders to bulk magnets is made easier by the platelet shape, which allows particles to be readily orientated and maximizes coercive field. Platelets can be piled up to achieve a similar outcome. Interparticle interactions in such a scenario influence the reduction of the internal field of platelets, which can enhance the magnetic characteristics.

(b) Managing the hard ferrite structure's doping:

PMs are frequently made from hard-magnetic ferrites with the magnetoplumbite structure. Kojima evaluated the advancements made in this field up to the early 1980s [83]But before the most recent overviews by Pullar [84] [85] Mahmood, and Lisjak et al [86], there weren't many reviews in the field. In general, the doping of M-type ferrites is intended to modify the inherent magnetic structure of this magneto-plumbite crystal, where the occupancy of five sites and their magnetic coupling via oxygen-driven superexchange interactions control magnetic characteristics. Because the spin configuration (high spin, low spin, or intermediate spin) influences the net magnetic moment and the local anisotropy of an ion, such design should consider that the spin and orbital moments of the cations rely on the site and charge distribution [87]. Various substitute possibilities can be taken into consideration within this framework. The first is to alter the overall magnetization. An alternative method is to increase the magnetocrystalline anisotropy locally by altering the crystal and chemical structures or by contributing the orbital moment. Generally speaking, it has been investigated to replace every ion found in the structure [84][83][85]. Though altering even the oxygen anions has been attempted, the most popular method takes into account the substitution of cations [83]. We employed technical-grade powders with a purity of 95+ % as our basic ingredients. Solid-state combustion was used to create ferrites, as previously mentioned. The dopant (La_2O_3 or CeO_2) was either added to the combustion products during grinding or combined with $BaCO_3$ ($SrCO_3$, PbO), Fe_2O_3, and Fe powders using ball milling. Synthesis was done in a quartz reactor with oxygen flowing through it in both instances [88].

(C) Substitution of non-magnetic cations for iron:

If non-magnetic atoms such as Al^{3+} and Ti^{2+} replace Fe in the spin-down sites, increasing the net moment, an increase in magnetization might be achieved. Nevertheless, this also results in a weakening of the exchange contacts, which can lower the room temperature magnetization, lower the Curie temperature, or weaken or alter the anisotropy symmetry [83].

Replacement of Fe by magnetic ions: For the first target, Fe^{3+} and Mn^{2+} are the 3d transition metal ions with the highest magnetic moments, whereas heavier rare earth ions have even higher magnetic moments.

As a result, doping with other 3D metals may enhance overall magnetization if ions occupy spin-down sites. To promote magnetocrystalline anisotropy, the replacement of ions with spin-orbit contributions might be the primary technique. However, except in a few circumstances, the great symmetry of the octahedral and tetrahedral sites reduces the orbital moment. As a result, occupancy of the bipyramidal 2b site is the desired outcome [87].

Substitution of Ba^{2+} or Sr^{2+} ions: Non-magnetic ions such as La^{2+}, Ca^{2+}, or Ag^{+}, as well as rare earth ions RE^{3+} [89] and others, alter the crystal structure, hence altering exchange interactions and magnetic anisotropies. For example, the slightly greater magnetic anisotropy of SrF (K_1 = 35 kJ m^{-3}) compared with BaF (K_1 = 32.5 kJ m^{-3}) is connected with the smaller size of Sr^{2+} (1.13 Å) than Ba^{2+} (1.35 Å). This is explained by the lower cell size, which results in a shorter Fe-O distance at the 2b sites, increasing the crystal field, zero-field splitting of Fe^{3+}, and magnetic anisotropy.

(D) Doping to make the magnetization stronger

There have been many attempts to dope M-hexaferrites in order to enhance their magnetization: the substitution encompasses several (magnetic and non-magnetic) component parts, one magnetic element, or one non-magnetic element. In accordance with the initio calculations of Dixit et al.[90], Bi, Sb, Sn, and Sc ions can increase magnetism. But as of yet, no experimental finding has shown a rise in magnetization. Numerous studies have been conducted on the Al^{3+} situation, but to no avail. The process of the creation of magnetic BaF doped with Ni produced by sol-gel was examined by Wang et al [91]. The only study that indicates an improvement for a single magnetic cation. For x = 0.8, they discovered a specific magnetization of 101 A m2 kg^{-1}. The authors propose that the presence of Fe^{2+} in $4f_1$ and 4f sites, along with Ni^{2+} occupancy of $4f_2$ spin-down sites, is the genesis.

Using the generic formula (Sr) $BaFe_{12-2x}Y_xZ_xO_{19}$, where Y and Z are different cations, injecting with several cations seems more promising. To ensure charge neutrality, Fe^{3+} is frequently substituted with equal quantities of divalent and tetravalent cations, and the replacement is frequently carried out using non-magnetic ions (paramagnetic or diamagnetic). Zn^{2+} doping in combination with additional diamagnetic ions, such as Ti , Zr , Sn , Nb , V , Sb , La , or with paramagnetic Ni cations, produced ferrites with σS ranging from 75 to 110 A m^2 kg^{-1}, resulting in larger σ_s. Typically, it was found that neither the specific magnetization nor the net magnetization showed monotonic trends with doping. In Zn^{2+} and Ti^{4+} doped BaF produced by coprecipitation, Wartewig et al. [92] demonstrate that the magnetization initially rises at low temperatures before falling beyond a doping of 0.4. Other compositions have also shown the augmentation of the magnetism. In $BaFe_{12-2x}Al_xCr_xO_{19}$ generated by auto combustion sol–gel, Trudel et al. [93] investigated the twofold substitution of Al^{3+} and Cr^{3+} cations. In comparison to the analogous BaF (81 A m^2 kg^{-1}), the doped ferrite exhibits a similar mass density and an exact magnetization of 88 A m^2 kg^{-1} at x = 0.4. The magnetization improvement does not have a linear dependence. Doping BaF and SrF with non-magnetic Ti^{2+} and Ru^{4+} cations was studied by Bsoul et al. There is a wide maximum in the magnetization versus doping in the two oxides. For both undoped oxides, the σ_s with replacement of x = 0.2 can reach up to 10% about values of about 60 A m^2 kg^{-1}. The spin breakdown $4f_2$ and $4f_1$ sites and the spin forward 2a and 2b sites, for x values up to 0.2, and the 12k site, for x > 0.2, are both replaced by Ti^{2+} and Ru^{4+} ions, according to Mössbauer spectroscopic research. The sole noteworthy instance is the study on AlCr–BaF carried out by Trudel et al. [83]. The doped ferrite exhibits a higher specific magnetization (88 A m^2 kg^{-1}) and coercive field (318 kA m^{-1}) at x = 0.4 than the analogous magnetization (81 A m^2 kg^{-1}) and HC (127 kA m^{-1}) of BaF. The authors explain this improvement by pointing out that the doped ferrites' reduced particle size causes an increase in Hc because of their single-domain behavior.

6.2 . Hard Ferrites in mW communications devices:

These important attributes of ferrites, which include being low-cost and experiencing minimal loss in permittivity, make them suitable for use as mW absorbers. High resistivity and minimal eddy current losses have made them suitable core materials for electrical and telecommunications uses [94,95]. The absorber should have high impedance matching and R_L for effective functioning. Reflection of the incident EM waves from the surface of the material in wireless communications is determined by the RL parameter [96].

$$RL = 20 \log \left| \frac{z_{in} - z_0}{z_{in} + z_0} \right|$$

Z_{in} varies according to the material in the equation above. The closer the input impedance is to Z_0, the better the impedance matching, and the lower the reflection loss. The following formula defines Z_{in}.

$$z_{in} = z_0 \sqrt{\frac{\mu_r}{\varepsilon_r}} \tanh\left(j \frac{2\Pi f d}{c} \sqrt{\mu_r \varepsilon_r} \right)$$

The values of f and d are represented by the wave frequency and the thickness of the sample, respectively. The speed of light is denoted by c, while the imaginary unit is denoted by j. Z_{in}/Z_0 is defined as the impedance matching, and guarantees that almost all the incident wave is absorbed by the substance.

The HF is anisotropic in nature, and they have a greater intrinsic magnetocrystalline anisotropy field compared to spinel and garnet ferrite. The HF is used for mW absorbers because it has a natural resonant frequency at GHz levels, due to its in-plane anisotropy [97]. As it was already discussed that hexagonal ferrite has magnto-plumbite structures and has a space group of P63/mmc, it exhibits unique magnetic characteristics, making them suitable material for mW absorbers and other applications [98]. They were discovered and characterized in the beginning years of the 1950s. Since then, their popularity has risen sharply because of their practical use. These are among the materials in high-frequency components that have attracted the most attention [99–101]. They have very high permeability [18], high saturation magnetization, high H_c [102,103], excellent chemical stability, high resistivity, and minimal loss of eddy current. This makes them highly suitable for applications such as radar absorbing materials [104,105]. The arrangement of basic units (S, R, and T) in their crystal structure forms is the main distinguishing factor among the different types of hexagonal ferrites.

Liu et al. studied the influence of Eu^{3+} on the performance of Sr-hexaferrite. The substitution of Eu^{3+} ions will increase the M_s and H_c of Sr-HFat at room temperature [106]. Alam et al. studied the Zn, Co, and Zr-doped M-type Ba-hexaferrite. They observed that the bandwidth and reflection loss (RL) of $BaZn_{0.5}Co_{0.5}ZrFe_{10}O_{19}$ HFare 8-12 GHz and -10 dB, respectively [107]. Chang et al. developed Ce-doped BaF($BaCe_{0.05}Fe_{11.95}O_{19}$) by employing the citrate sol-gel method. The material formed has an RL value of −37.4 dB at 12.8 GHz with 3.5 mm thickness in the 8-13 GHz frequency range [108].

7. CONCLUSION

Even though they have been around for a long time, hard ferrite remains one of the most significant magnetic materials for its distinct features of high Hc, chemical stability, high electrical resistivity, low cost, and environmental friendliness. This review is a summary of the various classes of hexaferrite, their crystal structure, magnetic properties, synthesis route, and application in high-frequency devices and PMs. Cation substitution, nano-structuring, and hard-soft magnetic nano-composites have been proven to enhance the magnetic properties of ferrite material to a certain extent, while decreasing the need for

expensive rare earth elements. The wide range of synthesis paths for the making of ferrite gives researchers flexibility in improving and varying the structural and magnetic properties of specific technological applications. The relevance of ferrite-based systems is growing with the ever-increasing requirement for sustainable materials in energy, transport, communications and the electronic industry. The application of ferrite in electrical mobility, wireless communication networks, and mWabsorbing material is all expected to significantly contribute to smart tourism applications. For future studies, advanced nanotechnology approaches, green synthesis method, and innovative composite designs, which could be used further to improve the energy product, Mr, and multifunctional properties of ferrite material.

Refrences:-

1. A. Mahanta, R. Samal, N.C. Sahu, Harnessing Renewable Energy to Advance Sustainable Tourism and Green Growth: A G20 Countries' Perspective, Energy RESEARCH LETTERS 7 (2026). https://doi.org/10.46557/001C.156401.
2. H. Rasool, S. Maqbool, Md. Tarique, The relationship between tourism and economic growth among BRICS countries: a panel cointegration analysis, Future Business Journal 2020 7:1 7 (2021) 1-. https://doi.org/10.1186/S43093-020-00048-3.
3. W. You, Y. Zhang, C.C. Lee, Climate Risk, Economic Stability, and Tourism: A Cross-Sectionally Dependent Heterogeneous Panel Causality Analysis, Energy RESEARCH LETTERS 2 (2021). https://doi.org/10.46557/001C.25723.
4. S.S. Rangarajan, C.K. Shiva, E.R. Collins, T. Senjyu, Electric Vehicle Motors Free of Rare-Earth Elements—An Overview, Machines 2025, Vol. 13, 13 (2025). https://doi.org/10.3390/MACHINES13080702.
5. I. Mohammed, J. Mohammed, A.K. Srivastava, Recent Progress in Hexagonal Ferrites Based Composites for Microwave Absorption, Crystal Research and Technology 58 (2023) 2200200. https://doi.org/10.1002/CRAT.202200200;PAGE:STRING:ARTICLE/CHAPTER.
6. J.R. Riba, C. López-Torres, L. Romeral, A. Garcia, Rare-earth-free propulsion motors for electric vehicles: A technology review, Renewable and Sustainable Energy Reviews 57 (2016) 367–379. https://doi.org/10.1016/J.RSER.2015.12.121.
7. O. Dehghani Dastjerdi, H. Shokrollahi, S. Mirshekari, A review of synthesis, characterization, and magnetic properties of soft spinel ferrites, Inorg. Chem. Commun. 153 (2023) 110797. https://doi.org/10.1016/J.INOCHE.2023.110797.
8. T.-H. Chang, T.-H. Chang, Ferrite Materials and Applications, Electromagnetic Materials and Devices (2019). https://doi.org/10.5772/INTECHOPEN.84623.
9. D. Sharma, Rohit, V. Singh, A. Dogra, M. Singh, Aluminium and praseodymium doped M-type hexaferrites for electric vehicle applications, Ceram. Int. 50 (2024) 24815–24822. https://doi.org/10.1016/J.CERAMINT.2024.04.217.
10. R. Duglet, A. Chauhan, D. Sharma, A. Thakur, M. Singh, Investigation on microwave absorption properties of bismuth ions doped barium hexaferrites, Journal of Materials Science: Materials in Electronics 35 (2024). https://doi.org/10.1007/S10854-024-12418-6.
11. M. Chandel, V.P. Singh, R. Jasrotia, K. Singha, R. Kumar, M. Chandel, V.P. Singh, R. Jasrotia, K. Singha, R. Kumar, A review on structural, electrical and magnetic properties of Y-type hexaferrites synthesized by different techniques for antenna applications and microwave absorbing characteristic

materials, AIMS Materials Science 2020 3:244 7 (2020) 244–268. https://doi.org/10.3934/MATERSCI.2020.3.244.

12. S.C. Tolani, A.R. Golhar, K.G. Rewatkar, A review of morphological, structural behaviour and technological applications of ferrites, AIP Conf. Proc. 2104 (2019). https://doi.org/10.1063/1.5100459/888717.
13. V. A., R. Jasrotia, An Overview of Hard Ferrites: Types and Structures, Materials Research Foundations 142 (2023) 1–34. https://doi.org/10.21741/9781644902318-1.
14. K.E. Latimer, H.B. Macdonald, A survey of the possible applications of ferrites, Proceedings of the IEE - Part II: Power Engineering 97 (1950) 257–267. https://doi.org/10.1049/PI-2.1950.0077.
15. S.C. Tolani, A.R. Golhar, K.G. Rewatkar, A review of morphological, structural behaviour and technological applications of ferrites, AIP Conf. Proc. 2104 (2019). https://doi.org/10.1063/1.5100459/888717.
16. A. Verma, P. Pandeyb, P. Sharma, Strontium ferrite permanent magnet-An overview, Indian Journal of Engineering & Materials Sciences 7 (n.d.) 364–369.
17. R. Jotania, Crystal structure, magnetic properties and advances in hexaferrites: A brief review, AIP Conf. Proc. 1621 (2014) 596–599. https://doi.org/10.1063/1.4898528.
18. H. Bayrakdar, Fabrication, magnetic and microwave absorbing properties of Ba2Co2Cr2Fe12O22 hexagonal ferrites, J. Alloys Compd. 674 (2016) 185–188. https://doi.org/10.1016/J.JALLCOM.2016.03.055.
19. T. Stijntjes, B. van Loon, T. Stijntjes, B. van Loon, Stijntjes, Theo, van Loon, Bob, Scanning Our Past from the Netherlands Early Investigations on Ferrite Magnetic Materials by J. L. Snoek and Colleagues of the Philips Research Laboratories Eindhoven, IEEEP 96 (2008) 900–904. https://doi.org/10.1109/JPROC.2008.917767.
20. A. Vedrtnam, K. Kalauni, S. Dubey, A. Kumar, A. Vedrtnam, K. Kalauni, S. Dubey, A. Kumar, A comprehensive study on structure, properties, synthesis and characterization of ferrites, AIMS Materials Science 2020 6:800 7 (2020) 800–835. https://doi.org/10.3934/MATERSCI.2020.6.800.
21. M.A. Gabal, E. Al-Mutairi, Y.M. Al Angari, A. Awad, A.A. Al-Juaid, A. Saeed, Synthesis, characterization, elastic, and electro-magnetic properties of MFe2O4 ferrites (M = Co2+, Ni2+, Cu2+, Mg2+, and Zn2+) via sucrose auto-combustion, Journal of Materials Research 2022 37:14 37 (2022) 2257–2270. https://doi.org/10.1557/S43578-022-00624-Z.
22. P. Sharma, G.K. Bhargava, S. Bhardwaj, I. Sharma, eds., Engineered Ferrites and Their Applications, (2023). https://doi.org/10.1007/978-981-99-2583-4.
23. M.D. Hossain, M.A. Hossain, S.S. Sikder, Hysteresis loop properties of rare earth doped spinel ferrites: A review, J. Magn. Magn. Mater. 564 (2022) 170095. https://doi.org/10.1016/J.JMMM.2022.170095.
24. C.M. Srivastava, M.J. Patni, N.G. Nanadikar, SIZE DEPENDENT FMR LINE-SHIFT AND LINE-WIDTH STUDIES IN POLYCRYSTALLINE FERRITES AND GARNETS, Le Journal de Physique Colloques 38 (1977) C1-267. https://doi.org/10.1051/JPHYSCOL:1977156.
25. C. Zhang, S. Feng, X. Kan, Y. Zhu, Z. Zhang, Y. Li, H. Tian, W. Sun, X. Liu, Structure and magnetic properties of Al3+ substituted M-type SrLaCo hexaferrite, J. Solid State Chem. 321 (2023) 123927. https://doi.org/10.1016/J.JSSC.2023.123927.
26. R.C. Pullar, Hexagonal ferrites: A review of the synthesis, properties and applications of hexaferrite ceramics, Prog. Mater. Sci. 57 (2012) 1191–1334. https://doi.org/10.1016/J.PMATSCI.2012.04.001.

27. I. Mohammed, J. Mohammed, A.U. Kende, A.M. Wara, Y.A. Aliero, U.Z. Magawata, A.B. Umar, A.K. Srivastava, Review on Y-type hexaferrite: Synthesis, characterization and properties, Applied Surface Science Advances 16 (2023) 100416. https://doi.org/10.1016/J.APSADV.2023.100416.
28. M. Sugimoto, The Past, Present, and Future of Ferrites, Journal of the American Ceramic Society 82 (1999) 269–280. https://doi.org/10.1111/J.1551-2916.1999.TB20058.X.
29. C. Granados-Miralles, M. Saura-Múzquiz, H.L. Andersen, Permanent Magnets Based on Hard Ferrite Ceramics, Ceramic Materials - Present and Future (2023). https://doi.org/10.5772/intechopen.1002234.
30. O.T.L. Traistaru, P. Shyam, M. Christensen, S.P. Madsen, Optimizing the energy product of exchange-coupled soft/hard Zn0.2Fe2.8O4/SrFe12O19magnets, J. Appl. Phys. 132 (2022). https://doi.org/10.1063/5.0103242/2837633.
31. H.R. Kirchmayr, Permanent magnets and hard magnetic materials, J. Phys. D Appl. Phys. 29 (1996) 2763. https://doi.org/10.1088/0022-3727/29/11/007.
32. F.J. Esper, MICROSTRUCTURE OF HARD FERRITES AND THEIR MAGNETIC PROPERTIES, Le Journal de Physique Colloques 38 (1977) C1-69. https://doi.org/10.1051/JPHYSCOL:1977114.
33. K. Elk, L. Jahn, Characteristics of Permanent Magnetic Coercivity with Application to Sintered Hard Ferrites, Physica Status Solidi (b) 168 (1991) 591–596. https://doi.org/10.1002/PSSB.2221680220;PAGE:STRING:ARTICLE/CHAPTER.
34. C. de Julián Fernández, C. Sangregorio, J. de la Figuera, B. Belec, D. Makovec, A. Quesada, Progress and prospects of hard hexaferrites for permanent magnet applications, J. Phys. D Appl. Phys. 54 (2021) 153001. https://doi.org/10.1088/1361-6463/ABD272.
35. J. Hlosta, K. Hrabovská, J. Rozbroj, J. Nečas, D. Žurovec, J. Diviš, O. Životský, Influence of calcination temperature and particle size distribution on the physical properties of SrFe12O19 and BaFe12O19 hexaferrite powders, Scientific Reports 2024 14:1 14 (2024) 17564-. https://doi.org/10.1038/s41598-024-67994-8.
36. Ch. Mamatha, M. Krishnaiah, B. Sreedhar, Enhancement Of Magnetic Properties Of Calcium Hexaferrites With Aluminium Substitution, Procedia Eng. 215 (2017) 130–135. https://doi.org/10.1016/J.PROENG.2017.11.001.
37. H. Nakamura, T. Waki, Y. Tabata, C. Mény, Co site preference and site-selective substitution in La–Co co-substituted magnetoplumbite-type strontium ferrites probed by 59Co nuclear magnetic resonance, Journal of Physics: Materials 2 (2019) 015007. https://doi.org/10.1088/2515-7639/AAF540.
38. C.C. Huang, C.C. Mo, G.M. Chen, H.H. Hsu, G.J. Shu, Investigation on the La Replacement and Little Additive Modification of High-Performance Permanent Magnetic Strontium-Ferrite, Processes 2021, Vol. 9, Page 1034 9 (2021) 1034. https://doi.org/10.3390/PR9061034.
39. M.R. Islam, M.K.R. Khan, M.S. Hossain, M.M. Rahman, M.M. Haque, M. Aliuzzaman, M.K. Alam, M.S.I. Sarker, Structural, thermodynamic, and magnetic properties of SrFe 12 O 19 hexaferrite modified by co-substitution of Cu and Gd, RSC Adv. 14 (2024) 7314–7328. https://doi.org/10.1039/D3RA08878B.
40. H. Han, Y. Luo, Y. Jia, N. Hasan, C. Liu, A review on SnFe2O4 and their composites: Synthesis, properties, and emerging applications, Progress in Natural Science: Materials International 32 (2022) 517–527. https://doi.org/10.1016/J.PNSC.2022.09.005.

41. T. Dippong, E.A. Levei, O. Cadar, Recent Advances in Synthesis and Applications of MFe2O4 (M = Co, Cu, Mn, Ni, Zn) Nanoparticles, Nanomaterials 2021, Vol. 11, Page 1560 11 (2021) 1560. https://doi.org/10.3390/NANO11061560.
42. M. Imran Din, F. Rafique, M.S. Hussain, H. Arslan Mehmood, S. Waseem, Recent developments in the synthesis and stability of metal ferrite nanoparticles, Sci. Prog. 102 (2019) 61–72. https://doi.org/10.1177/0036850419826799;WEBSITE:WEBSITE:SAGE;JOURNAL:JOURNAL:SCIA;WGROUP:STRING:PUBLICATION.
43. L. Kumar, P. Kumar, A. Narayan, M. Kar, Rietveld analysis of XRD patterns of different sizes of nanocrystalline cobalt ferrite, International Nano Letters 2013 3:1 3 (2013) 8-. https://doi.org/10.1186/2228-5326-3-8.
44. I. Mohammed, J. Mohammed, A.K. Srivastava, Recent Progress in Hexagonal Ferrites Based Composites for Microwave Absorption, Crystal Research and Technology 58 (2023) 2200200. https://doi.org/10.1002/CRAT.202200200;PAGE:STRING:ARTICLE/CHAPTER.
45. S. Fayazzadeh, M. Khodaei, Salt-assisted combustion synthesis of cobalt ferrite nanoparticles; magnetic properties and cation distribution measurement by XRD analysis, Journal of Ultrafine Grained and Nanostructured Materials 52 (2019) 69–77. https://doi.org/10.22059/JUFGNSM.2019.01.07.
46. M.K.A. Kar, F. Manteghi, M. Ghahari, M.K.A. Kar, F. Manteghi, M. Ghahari, Microwave assisted sol-gel auto-combustion synthesis of NiCuFe2O4 nanoparticles using citric acid as an organic chelating agent: structural and optical studies, (2015) c005. https://doi.org/10.3390/ECSOC-19-C005.
47. S.C. Tolani, A.R. Golhar, K.G. Rewatkar, A review of morphological, structural behaviour and technological applications of ferrites, AIP Conf. Proc. 2104 (2019). https://doi.org/10.1063/1.5100459/888717.
48. D. Bokov, A. Turki Jalil, S. Chupradit, W. Suksatan, M. Javed Ansari, I.H. Shewael, G.H. Valiev, E. Kianfar, Nanomaterial by Sol-Gel Method: Synthesis and Application, Advances in Materials Science and Engineering 2021 (2021) 5102014. https://doi.org/10.1155/2021/5102014.
49. M.A. Almessiere, A. V. Trukhanov, Y. Slimani, K.Y. You, S. V. Trukhanov, E.L. Trukhanova, F. Esa, A. Sadaqati, K. Chaudhary, M. Zdorovets, A. Baykal, Correlation Between Composition and Electrodynamics Properties in Nanocomposites Based on Hard/Soft Ferrimagnetics with Strong Exchange Coupling, Nanomaterials 2019, Vol. 9, Page 202 9 (2019) 202. https://doi.org/10.3390/NANO9020202.
50. Powder Technology, (2018).
51. A.A. Ati, A.H. Abdalsalam, A.S. Hasan, Thermal, microstructural and magnetic properties of manganese substitution cobalt ferrite prepared via co-precipitation method, Journal of Materials Science: Materials in Electronics 2021 32:3 32 (2021) 3019–3037. https://doi.org/10.1007/S10854-020-05053-4.
52. R. Baladi, K. Gheisari, Structural, Magnetic and Dielectric Properties of Nanocrystalline (M = Li and Mg) Ferrites Synthesized via EDTA/EG Assisted Sol-Gel Method, Transactions of the Indian Ceramic Society 78 (2019) 195–203. https://doi.org/10.1080/0371750X.2019.1671901.
53. P. Sharma, G.K. Bhargava, S. Bhardwaj, I. Sharma, eds., Engineered Ferrites and Their Applications, (2023). https://doi.org/10.1007/978-981-99-2583-4.

54. A.R.F. Pacheco, B.D. Cardoso, A. Pires, A.M. Pereira, J.P. Araújo, V.M. Carvalho, R.O. Rodrigues, P.J.G. Coutinho, T. Castelo-Grande, P.A. Augusto, D. Barbosa, R.A. Lima, S.F.C.F. Teixeira, A.R.O. Rodrigues, E.M.S. Castanheira, Development of pH-Sensitive Magnetoliposomes Containing Shape Anisotropic Nanoparticles for Potential Application in Combined Cancer Therapy, Nanomaterials 13 (2023) 1051. https://doi.org/10.3390/NANO13061051/S1.
55. B.C. Ribeiro, C.A.R. Alvarez, B.C. Alves, J.M. Rodrigues, M.J.R.P. Queiroz, B.G. Almeida, A. Pires, A.M. Pereira, J.P. Araújo, P.J.G. Coutinho, A.R.O. Rodrigues, E.M.S. Castanheira, Development of Thermo- and pH-Sensitive Liposomal Magnetic Carriers for New Potential Antitumor Thienopyridine Derivatives, Materials 2022, Vol. 15, Page 1737 15 (2022) 1737. https://doi.org/10.3390/MA15051737.
56. D. Toledo, Cobalt Ferrite Nanoparticles Fabricated via Co-precipitation in Air: Overview of Size Control and Magnetic Properties, (2015). https://doi.org/10.25148/ETD.FIDC000195.
57. G. Sedaghati-Jamalabad, M.M. Bagheri-Mohagheghi, Influence of synthesis route on structural properties of SnFe2O4 spinel phase via methods of co-precipitation, sol–gel and solvothermal: morphology, phase analysis, crystallite size and lattice strain, Discover Applied Sciences 2024 6:4 6 (2024) 202-. https://doi.org/10.1007/S42452-024-05873-7.
58. S. Neeradi, L.R. Kotha, Effect of Y and Mn on structural, morphological, optical, magnetic properties, photocatalytic and biological activity of cobalt Nano ferrites by citrate gel auto combustion method, Polyhedron 281 (2025) 117726. https://doi.org/10.1016/J.POLY.2025.117726.
59. A.K. Singh, T.C. Goel, R.G. Mendiratta, Low-temperature synthesis of Mno0.2Ni0.2Zn 0.6Fe2O4 ferrites by citrate precursor method and study of their properties, Physica Status Solidi A Appl. Res. 201 (2004) 1453–1457. https://doi.org/10.1002/PSSA.200306775;REQUESTEDJOURNAL:JOURNAL:1521396X;WGROUP:STRING:PUBLICATION.
60. A. Pasko, F. Mazaleyrat, M. LoBue, V. Loyau, V. Basso, M. Küpferling, C.P. Sasso, L. Bessais, Magnetic and structural characterization of nanosized BaCoxZn2−xFe16O27 hexaferrite in the vicinity of spin reorientation transition, J. Phys. Conf. Ser. 303 (2011) 012045. https://doi.org/10.1088/1742-6596/303/1/012045.
61. S.F. Shaikh, M. Ubaidullah, R.S. Mane, A.M. Al-Enizi, Types, Synthesis methods and applications of ferrites, Spinel Ferrite Nanostructures for Energy Storage Devices (2020) 51–82. https://doi.org/10.1016/B978-0-12-819237-5.00004-3.
62. J.A. Hwang, M. Choi, H.S. Shin, B.K. Ju, M.P. Chun, Structural and Magnetic Properties of NiZn Ferrite Nanoparticles Synthesized by a Thermal Decomposition Method, Applied Sciences 2020, Vol. 10, Page 6279 10 (2020) 6279. https://doi.org/10.3390/APP10186279.
63. J. Liu, M. Walmer, M. Jasinski, Modern Sm-Co permanent magnets, Modern Permanent Magnets (2022) 113–134. https://doi.org/10.1016/B978-0-323-88658-1.00001-7.
64. [J.J. Becker, Rare-Earth-Compound Permanent Magnets, J. Appl. Phys. 41 (1970) 1055–1064. https://doi.org/10.1063/1.1658811.
65. E.P. Wohlfarth, Magnetic properties of single domain ferromagnetic particles, J. Magn. Magn. Mater. 39 (1983) 39–44. https://doi.org/10.1016/0304-8853(83)90393-1.
66. C. Kittel, Physical Theory of Ferromagnetic Domains, Rev. Mod. Phys. 21 (1949) 541. https://doi.org/10.1103/RevModPhys.21.541.

67. C. de Julián Fernández, C. Sangregorio, J. de la Figuera, B. Belec, D. Makovec, A. Quesada, Progress and prospects of hard hexaferrites for permanent magnet applications, J. Phys. D Appl. Phys. 54 (2021) 153001. https://doi.org/10.1088/1361-6463/ABD272.
68. C. Kittel, Physical Theory of Ferromagnetic Domains, Rev. Mod. Phys. 21 (1949) 541. https://doi.org/10.1103/RevModPhys.21.541.
69. O. Kitakami, K. Goto, T. Sakurai, A Study of the Magnetic Domains of Isolated Fine Particles of Ba Ferrite, Jpn. J. Appl. Phys. 27 (1988) 2274. https://doi.org/10.1143/JJAP.27.2274.
70. T. Hirayama, Q. Ru, T. Tanji, A. Tonomura, Observation of magnetic-domain states of barium ferrite particles by electron holography, Appl. Phys. Lett. 63 (1993) 418–420. https://doi.org/10.1063/1.110011.
71. B.T. SHIRK, W.R. BUESSEM, Magnetic Properties of Barium Ferrite Formed by Crystallization of a Glass, Journal of the American Ceramic Society 53 (1970) 192–196. https://doi.org/10.1111/J.1151-2916.1970.TB12069.X.
72. E.P. Wohlfarth, Magnetic properties of single domain ferromagnetic particles, J. Magn. Magn. Mater. 39 (1983) 39–44. https://doi.org/10.1016/0304-8853(83)90393-1.
73. Z.B. Guo, W.P. Ding, W. Zhong, J.R. Zhang, Y.W. Du, Preparation and magnetic properties of SrFe12O19 particles prepared by the salt-melt method, J. Magn. Magn. Mater. 175 (1997) 333–336. https://doi.org/10.1016/S0304-8853(97)00206-0.
74. J.M. González, C. De Julián, A.K. Giri, S. Castro, M. Gayoso, J. Rivas, Magnetic viscosity and microstructure: Particle size dependence of the activation volume, J. Appl. Phys. 79 (1996) 5955–5957. https://doi.org/10.1063/1.362118.
75. Y. Chen, W. Yang, D.N. Lambeth, M.H. Kryder, Incoherent rotation in barium ferrite thin film recording media, IEEE Trans. Magn. 33 (1997) 2998–3000. https://doi.org/10.1109/20.617823.
76. O. Kubo, T. Ido, H. Yokoyama, Y. Koike, Particle size effects on magnetic properties of BaFe12−2xTixCoxO19 fine particles, J. Appl. Phys. 57 (1985) 4280–4282. https://doi.org/10.1063/1.334585.
77. T. Chang, J.G. Zhu, J.H. Judy, Method for investigating the reversal properties of isolated barium ferrite fine particles utilizing magnetic force microscopy (MFM), J. Appl. Phys. 73 (1993) 6716–6718. https://doi.org/10.1063/1.352512.
78. S. Tyagi, R.C. Agarwala, V. Agarwala, Microwave Absorption and Magnetic Studies of Strontium Hexaferrites Nanoparticles Synthesized by Modified Flux Method, Journal of Nano Research 10 (2010) 19–27. https://doi.org/10.4028/WWW.SCIENTIFIC.NET/JNANOR.10.19.
79. A. Ghasemi, V. Šepelák, X. Liu, A. Morisako, Mössbauer spectroscopy and magnetic susceptibility studies of Cr–Al substituted strontium ferrite particles, J. Appl. Phys. 107 (2010). https://doi.org/10.1063/1.3339004/342570.
80. A. Lasoialfari, M. Filibian, C. Sangregorio, P. Carretta, In vivo biomedical applications of magnetic resonance and magnetic materials, La Rivista Del Nuovo Cimento 2013 36:6 36 (2013) 211–271. https://doi.org/10.1393/NCR/I2013-10089-8.
81. J. Dho, E.K. Lee, J.Y. Park, N.H. Hur, Effects of the grain boundary on the coercivity of barium ferrite BaFe12O19, J. Magn. Magn. Mater. 285 (2005) 164–168. https://doi.org/10.1016/J.JMMM.2004.07.033.

82. H. Kojima, Chapter 5 Fundamental properties of hexagonal ferrites with magnetoplumbite structure, Handbook of Ferromagnetic Materials 3 (1982) 305–391. https://doi.org/10.1016/S1574-9304(05)80091-4.
83. R.C. Pullar, Hexagonal ferrites: A review of the synthesis, properties and applications of hexaferrite ceramics, Prog. Mater. Sci. 57 (2012) 1191–1334. https://doi.org/10.1016/J.PMATSCI.2012.04.001.
84. C. de Julián Fernández, C. Sangregorio, J. de la Figuera, B. Belec, D. Makovec, A. Quesada, Progress and prospects of hard hexaferrites for permanent magnet applications, J. Phys. D Appl. Phys. 54 (2021) 153001. https://doi.org/10.1088/1361-6463/ABD272.
85. D. Lisjak, A. Mertelj, Anisotropic magnetic nanoparticles: A review of their properties, syntheses and potential applications, Prog. Mater. Sci. 95 (2018) 286–328. https://doi.org/10.1016/J.PMATSCI.2018.03.003.
86. G.F. Dionne, Magnetic oxides, Magnetic Oxides (2009) 1–466. https://doi.org/10.1007/978-1-4419-0054-8/SAVE-RESEARCH.
87. K.S. Martirosyan, N.S. Martirosyan, A.E. Chalykh, La3+ and Ce3+ doping of hard-magnetic ferrites, Inorganic Materials 40 (2004) 527–532. https://doi.org/10.1023/B:INMA.0000027601.25937.82/METRICS.
88. S. Ounnunkad, Improving magnetic properties of barium hexaferrites by La or Pr substitution, Solid State Commun. 138 (2006) 472–475. https://doi.org/10.1016/J.SSC.2006.03.020.
89. V. Dixit, S.G. Kim, J. Park, Y.K. Hong, Effect of ionic substitutions on the magnetic properties of strontium hexaferrite: A first principles study, AIP Adv. 7 (2017). https://doi.org/10.1063/1.4995309/22415.
90. M. Wang, Q. Xu, J. Liu, Z. Wang, N. Ma, P. Du, Extra up-spin magnetic moments and extraordinary high saturation magnetization of Ni2+ doped barium ferrite in 4f2 site, Mater. Res. Express 6 (2019) 086104. https://doi.org/10.1088/2053-1591/AB1A0C.
91. P. Wartewig, M.K. Krause, P. Esquinazi, S. Rösler, R. Sonntag, Magnetic properties of Zn- and Ti-substituted barium hexaferrite, J. Magn. Magn. Mater. 192 (1999) 83–99. https://doi.org/10.1016/S0304-8853(98)00382-5.
92. T.T. Carol Trudel, J. Mohammed, H.Y. Hafeez, B.H. Bhat, S.K. Godara, A.K. Srivastava, Structural, Dielectric, and Magneto-Optical Properties of Al-Cr Substituted M-Type Barium Hexaferrite, Physica Status Solidi (A) Applications and Materials Science 216 (2019) 1800928. https://doi.org/10.1002/PSSA.201800928;WGROUP:STRING:PUBLICATION.
93. M. Banerjee, A. Mukherjee, S. Chakrabarty, S. Basu, M. Pal, Bismuth-Doped Nickel Ferrite Nanoparticles for Room Temperature Memory Devices, ACS Appl. Nano Mater. 2 (2019) 7795–7802. https://doi.org/10.1021/ACSANM.9B01828.
94. I. Ali, M. Islam, M. Ashiq, M. Iqbal, H.K.-… and magnetic materials, undefined 2014, Role of grain boundaries in the conduction of Eu–Ni substituted Y-type hexaferrites, ElsevierI Ali, MU Islam, MN Ashiq, MA Iqbal, HM Khan, G MurtazaJournal of Magnetism and Magnetic Materials, 2014•Elsevier (n.d.). https://www.sciencedirect.com/science/article/pii/S0304885314002406 (accessed June 6, 2026).
95. I. Mohammed, J. Mohammed, A.K. Srivastava, Recent Progress in Hexagonal Ferrites Based Composites for Microwave Absorption, Crystal Research and Technology 58 (2023) 2200200. https://doi.org/10.1002/CRAT.202200200;PAGE:STRING:ARTICLE/CHAPTER.

96. Y. He, R. Wang, X. Wu, C. Tang, J. Qian, P. Zuo, Q. Zhuang, X. Liu, The combined sol-gel and ascorbic acid reduction strategy enabling Ba2Co2Fe12O22 hexaferrite/graphene composite with enhanced microwave absorption ability, Mater. Res. Bull. 174 (2024) 112721. https://doi.org/10.1016/J.MATERRESBULL.2024.112721.
97. A. Ghasemi, A. Hossienpour, A. Morisako, A. Saatchi, M. Salehi, Electromagnetic properties and microwave absorbing characteristics of doped barium hexaferrite, J. Magn. Magn. Mater. 302 (2006) 429–435. https://doi.org/10.1016/J.JMMM.2005.10.006.
98. J. Mohammed, T. Tekou Carol, H.Y. Hafeez, D. Basandrai, G.R. Bhadu, S.K. Godara, S.B. Narang, A.K. Srivastava, Lightweight SrM/CCTO/rGO nanocomposites for optoelectronics and Ku band microwave absorption, Journal of Materials Science: Materials in Electronics 2019 30:4 30 (2019) 4026–4040. https://doi.org/10.1007/S10854-019-00690-W.
99. L. Qiao, L. You, J. Zheng, L. Jiang, J.S.-J. of magnetism and, undefined 2007, The magnetic properties of strontium hexaferrites with La–Cu substitution prepared by SHS method, ElsevierL Qiao, L You, J Zheng, L Jiang, J ShengJournal of Magnetism and Magnetic Materials, 2007•Elsevier (n.d.). https://www.sciencedirect.com/science/article/pii/S0304885307006488 (accessed June 6, 2026).
100. A. Ghasemi, V. Šepelák, X. Liu, A. Morisako, Microwave absorption properties of Mn-Co-Sn doped barium ferrite nanoparticles, IEEE Trans. Magn. 45 (2009) 2456–2459. https://doi.org/10.1109/TMAG.2009.2018611.
101. N. Tran, Y.J. Choi, T.L. Phan, D.S. Yang, B.W. Lee, Electronic structure and magnetic and electromagnetic wave absorption properties of BaFe12-xCoxO19 M-type hexaferrites, Current Applied Physics 19 (2019) 1343–1348. https://doi.org/10.1016/J.CAP.2019.08.023.
102. A. Jain, Y.G. Wang, N. Wang, Y. Li, F.L. Wang, Existence of heterogeneous phases with significant improvement in electrical and magnetoelectric properties of BaFe12O19/BiFeO3 multiferroic ceramic composites, Ceram. Int. 45 (2019) 22889–22898. https://doi.org/10.1016/J.CERAMINT.2019.07.332.
103. Y. Slimani, B. Unal, M.A. Almessiere, A. Demir Korkmaz, A. Baykal, Investigation of AC susceptibility, dielectric and electrical properties of Tb–Tm co-substituted M-type Sr hexaferrites, Mater. Chem. Phys. 260 (2021) 124162. https://doi.org/10.1016/J.MATCHEMPHYS.2020.124162.
104. M. Shahbaz, I. Sadiq, M.M.H. Butt, A. Basit Javaid, M. Idrees, S. Hussain, F. Sadiq, S. Riaz, S. Naseem, H.M. Khan, Peculiar magnetic behavior and structural, electrical, dielectric properties of substituted R-type hexagonal ferrites, J. Magn. Magn. Mater. 499 (2020) 166309. https://doi.org/10.1016/J.JMMM.2019.166309.
105. R. Topkaya, I. Auwal, A. Baykal, Effect of temperature on magnetic properties of BaYxFe12−xO19 hexaferrites, Ceram. Int. 42 (2016) 16296–16302. https://doi.org/10.1016/J.CERAMINT.2016.07.178.
106. C. Liu, X. Kan, X. Liu, S. Feng, J. Hu, W. Wang, K.M. Ur Rehman, M. Shezad, Influence of the Eu substitution on the structure and magnetic properties of the Sr-hexaferrites, Ceram. Int. 46 (2020) 171–179. https://doi.org/10.1016/J.CERAMINT.2019.08.245.
107. R.S. Alam, M. Moradi, M. Rostami, H. Nikmanesh, R. Moayedi, Y. Bai, Structural, magnetic and microwave absorption properties of doped Ba-hexaferrite nanoparticles synthesized by co-precipitation method, J. Magn. Magn. Mater. 381 (2015) 1–9. https://doi.org/10.1016/J.JMMM.2014.12.059.

108. S. Chang, S. Kangning, C.P.-J. of M. and Magnetic, undefined 2012, Microwave absorption properties of Ce-substituted M-type barium ferrite, ElsevierS Chang, S Kangning, C PengfeiJournal of Magnetism and Magnetic Materials, 2012•Elsevier (n.d.). https://www.sciencedirect.com/science/article/pii/S0304885311006937 (accessed June 6, 2026).